Identification and characterisation of Stx5 a novel interactor of VLDL-R affecting its intracellular trafficking and processing

Dissertation

zur Erlangung des Grades

“Doktor der Naturwissenschaften”

am Fachbereich Biologie

der Johannes Gutenberg-Universität Mainz

von

Timo Wagner

geboren am 27. Januar 1981 in Worms

Mainz, im April 2013

Dekan:

1. Berichterstatter:

2. Berichterstatter:

Tag der mündlichen Prüfung: 27.06.2013

TABLE OF CONTENTS

Abbreviations

α-MEM	Alpha Minimum Essential Medium
aa	Amino acid
ADAM	A disintegrin and metalloproteases
ADE	Adenine
ANOVA	Analysis of variance
ApoE	Apolipoprotein E
ApoER2	Apolipoprotein E receptor 2
APP	Amyloid precursor protein
ARH	Autosomal recessive hypercholesterolemia
BFA	Brefeldin A
CTF	C-terminal fragment
Co-IP	Co-immunoprecipitation
COP	Coatamer protein
C_{ub}	C-terminal fragment of ubiquitin
Dab1	Disabled 1
DMEM	Dulbecco's Modified Eagle Medium
EGF	Epidermal growth factor
Endo H	Endoglycosidase H
ER	Endoplasmic reticulum
ERGIC/VTC	ER-Golgi intermediate compartment/vesicular tubular carriers
esiRNA	Endoribonuclease-prepared silencing RNA
GST	Glutathione S-transferase
HEK	Human embryonic kidney
HIS	Histidine
IC	Immunocytochemistry
ICD	Intracellular domain
IP	Immunoprecipitation
IPTG	Isopropyl-*β*-D-thiogalactopyranosid
kDa	Kilo Dalton
KLH	Keyhole limpet hemocyanin
LDL-R	Low density lipoprotein-receptor

LRP	low density lipoprotein receptor-related protein
mbSUS	Mating-based Split Ubiquitin System
mLRP1 IV	Mini-receptor LRP1 domain IV
mRNA	Messenger RNA
N_{ub}	N-terminal fragment of ubiquitin
PS	Presenilin
PTB	Phosphotyrosine binding
RT	Room temperature
SNARE	N-ethylmaleimide-sensitive factor-attachment protein receptor
SNX17	Sortin nexin 17
Stx	Syntaxin
sVLDL-R	Soluble very low density lipoprotein-receptor
TF	Transcription factor
TGN	*Trans*-Golgi network
TMD	Transmembrane domain
UBP	Ubiquitin specific protease
VLDL	Very low density lipoprotein
VLDL-R	Very low density lipoprotein-receptor
WB	Western blot

1 INTRODUCTION

1.1 The very low density lipoprotein (VLDL)-receptor

The very low density lipoprotein (VLDL)-receptor (VLDL-R), a type I transmembrane glycoprotein is part of the low density lipoprotein (LDL)-receptor (LDL-R) gene family (Figure 1), whose members were originally considered as recycling cell surface receptors for the uptake and lysosomal degradation of extracellular ligands like ApoE containing lipoproteins (Krieger and Herz, 1994). Like all members of this family, VLDL-R consists of a large ectodomain including cysteine-rich repeats for ligand binding, epidermal growth factor (EGF) type cysteine-rich repeats and one or more YWTD domains, a single transmembrane domain (TMD) and a short cytoplasmic tail harbouring an Asparagine-Proline-X-Tyrosine (NPxY) internalisation motif, whereby x refers to any amino acid. Additionally, like its structurally most closely related gene family members LDL-R and the Apolipoprotein E receptor 2 (ApoER2), the VLDL-receptor contains a serine and threonine-rich extracellular region which is important for the proteolytic processing of the ectodomain (Magrane et al., 1999). This so called “ectodomain shedding“ of the cell surface resident form of VLDL-R generates a secreted soluble form of VLDL-R (sVLDL-R) and cell-associated C-terminal fragments (CTFs), and is usually carried out by extracellular, membrane bound metalloproteinases (A Disintegrin and Metalloproteinase, ADAM) (Rebeck et al., 2006). Moreover, the CTFs can undergo further processing by γ-secretase (Rebeck et al., 2006), a multi-subunit protease complex whose most renowned substrates amongst others are NOTCH and the amyloid precursor protein (APP) (Kaether et al., 2006).

VLDL-R is mainly expressed in extrahepatic tissue like skeletal muscle, heart, brain and endothelial cells of major blood vessels (Willnow et al., 1996; Wyne et al., 1996). However,

the receptor is rarely found in the liver, the major site of the very-low density lipoprotein (VLDL) catabolism. Therefore, its originally proposed function as mediator of the uptake of ApoE-rich VLDL particles within hepatic tissue is disputable. Indeed, inactivation of the VLDL-R gene in a mouse model did not lead to disturbed lipid homeostasis, but instead displayed defects in neuronal development comparable to those found in the reelin knockout mouse (Frykman et al., 1995; Trommsdorff et al., 1999). In this context, VLDL-R is regarded as important for the proper migration and layering of neurons in the cortex and cerebellum during brain development (D'Arcangelo et al., 1999; Hiesberger et al., 1999; Trommsdorff et al., 1999). In the early state of embryonic development, VLDL-R and ApoER2 cooperate in the transmission of the reelin signal and further transduction cascade. Both receptors simultaneously bind reelin with their ectodomains and subsequently induce tyrosine phosphorylation of disabled 1 (Dab1), which is capable of interacting with the NPxY motifs of both receptors through its phosphotyrosine binding (PTB) domain (Trommsdorff et al., 1998; Beffert et al., 2006). This tyrosine phosphorylation of Dab1 is essential for the further transmission of the reelin signal to induce proper neuronal migration. This certain role of VLDL-R in brain development not only shows that the receptor indeed has other functions than the endocytosis of extracellular cargo, but also highlights the importance of the intracellular binding of adaptor proteins to the cytoplasmic tail of VLDL-R.

1.2 The importance of intracellular adaptor proteins on the function of LDL-receptors

Protein-protein interactions are essential for the majority of biological functions. Intracellular adaptor proteins like Dab1 binding to intracellular domains of cell surface

receptors not only participate in processes like signal transduction but also influence trafficking and processing of lipoprotein receptors directly or by assembling to multi-protein complexes (Trommsdorff et al., 1998; Wagner and Pietrzik, 2012). For instance, in early

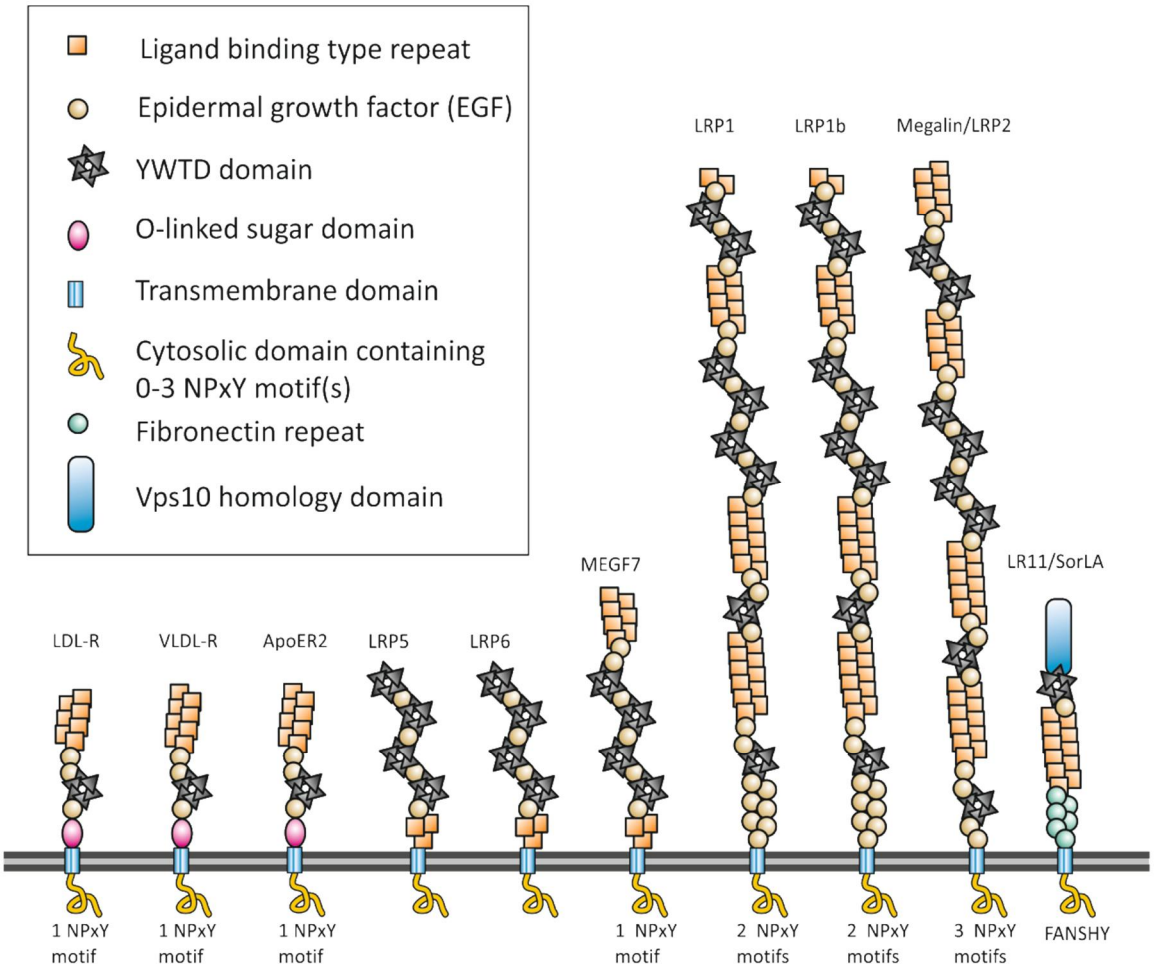

Figure 1 The LDL-receptor gene family. The LDL-receptor gene family comprises 7 core members and the three distantly related members LRP5, LRP6 and LR11/SorLA. The illustration presents the structural domain organisation of the receptors. Common for all members are ligand binding type repeats, epidermal growth factor (EGF) – homology domains and YWTD propeller domains important for pH-dependent release of receptor bound ligands into endosomal vesicles. Additionally, all LDL-receptors are characterised by a single membrane spanning region and a cytoplasmic tail containing one or more NPxY motifs (with the exception of LRP5 and LRP6 carrying no such a motif) representing both the endocytosis signal and the binding site for intracellular adaptor and scaffold proteins. LDL-R, VLDL-R and ApoER2 carry additional O-glycosylation motifs. SorLA comprises two additive domains not common with the characteristic structures of the family, one vacuolar protein-sorting 10 protein (Vps10p) domain and fibronectin repeats (modified from Wagner and Pietrzik, 2012).

endosomal compartments, the adaptor protein sortin nexin 17 (SNX17) was shown to interact with the NPxY motifs of LDL-R and the low density lipoprotein receptor-related protein (LRP) 1, suggesting a function for SNX17 in the basolateral sorting of the receptors (Burden et al., 2004; van Kerkhof et al., 2005). The autosomal recessive hypercholesterolemia (ARH) protein can influence endocytosis of LDL-receptors by associating them to the clathrin machinery (He et al., 2002; Mishra et al., 2002). It has been shown that LRP1 can modulate processing and trafficking of APP at the plasma membrane as well as in early secretory compartments (Ulery et al., 2000; Arelin et al., 2002; Pietrzik et al., 2002; Waldron et al., 2008). In this context, Fe65 serves as a mediating linker protein connecting both receptors to a tripartite complex (Kinoshita et al., 2001; Pietrzik et al., 2004). Since a similar complex can also be formed between APP, Fe65 and ApoER2 (Hoe et al., 2006; Hoe et al., 2006), it has recently been suggested that Fe65 might also act as an intracellular linker between VLDL-R and APP affecting trafficking and processing of both receptors (Dumanis et al., 2012). Moreover, the complex of Fe65 and VLDL-R CTFs seemed to translocated to the nucleus in a similar fashion as the earlier reported association of Fe65 with APP CTFs (Russo et al., 1998), suggesting a putative role for VLDL-R CTFs in transcriptional gene regulation.

1.3 The mating-based Split Ubiquitin System (mbSUS)

To identify new adaptor proteins which might influence VLDL-R function, trafficking and/or processing we performed a membrane-based yeast two-hybrid (YTH) screen (Johnsson and Varshavsky, 1994; Stagljar et al., 1998). The YTH system was developed in 1989 to study interactions between cytosolic proteins (Fields and Song, 1989). Since this method is based on the reconstitution of a transcription factor separated in a DNA-binding domain and a

transcripitional activation domain, the interaction assays are restricted to the nucleus. This fact presents a problem when studying interactions between membrane proteins, since they have to be portioned into small fragments and then re-localised to the nucleus. Contrary to the conventional YTH method, the "mating-based Split Ubiquitin System" (mbSUS) is not based on a transcriptional readout but on the reconstitution of ubiquitin, a small highly conserved protein which tags other proteins for degradation (Hershko, 2005). Proteins destined for proteasomal degradation are covalently attached with a chain of ubiquitin molecules and transported to the 26S proteasome for subsequent degradation. Ubiquitin itself is recycled from this mechanism by off-cleavage from the target proteins. This process is mediated by ubiquitin specific proteases (UBPs). The inventors of the method, Nils Jonsson and Alexander Varshavsky, found that yeast ubiquitin can be split into two halves, termed N_{ub} (N-terminal part of ubiquitin) and C_{ub} (C-terminal part of ubiquitin). When expressed separately, both parts remain only partially folded and consequently, are not recognised by UBPs. Contrary, co-expression of C_{ub} and N_{ub} within the same cell leads to efficient re-assembly of both halves into so-called "split-ubiquitin", which assumes natively folded ubiquitin due to their strong affinity to each other. The mbSUS now makes use of the fact that UBPs cannot recognise misfolded, modified or incomplete ubiquitin molecules (Johnsson and Varshavsky, 1994). The high affinity of wild-type N_{ub} (termed N_{ub}I due to an isoleucine at position 13 of the protein) to C_{ub} can be abolished by exchange of the isoleucine with a glycine (G). Consequently, this N_{ub}G displays almost no affinity to C_{ub} when co-expressed. As there is no re-assembly to split-ubiquitin, C_{ub} remains partially unfolded and is not recognised by UBPs. Johnsson and Varshavsky converted this into a protein complementation assay by fusing a membrane protein of interest X to C_{ub} and the artificial

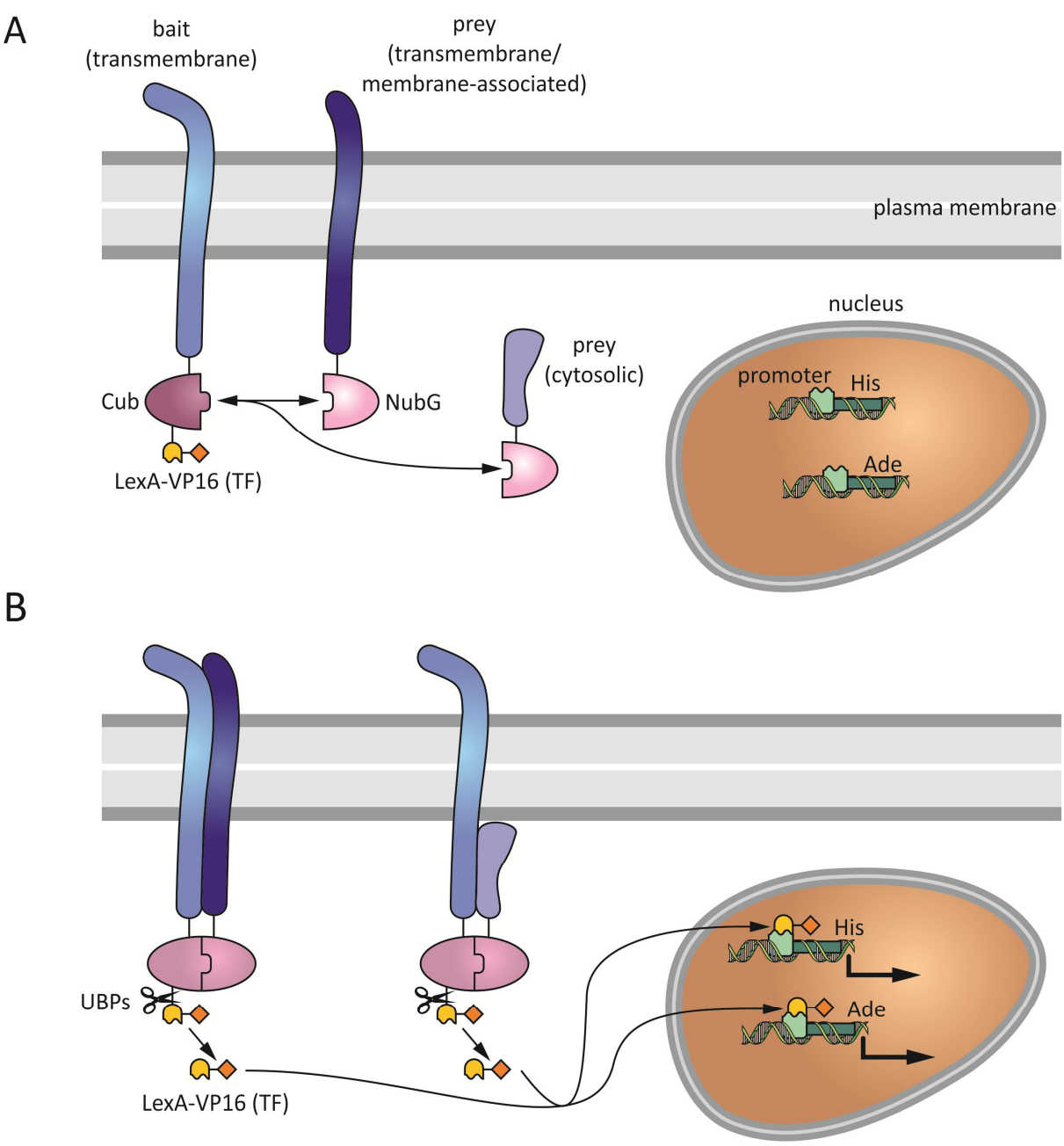

Figure 2 The mating-based Split Ubiquitin System (mbSUS). (A) In this modified YTH system a transmembrane protein (referred to as "bait"), e.g. a member of the LDL-receptor gene family, is fused to the C-terminal part of ubiquitin (C_{ub}). The potential "prey" protein is fused to the N-terminal part of ubiquitin carrying the isoleucine to glycine exchange at position 13 ($N_{ub}G$) and can either be transmembrane, membrane-associated or cytosolic. If bait and prey, do not interact with each other the artificial transcription factor (TF) LexA-VP16 is not cleaved off by ubiquitin specific proteases (UBPs). (B) Interaction between bait and prey forces $N_{ub}G$ and C_{ub} into close proximity, leading to re-assembling of the two separate parts into split-ubiquitin and subsequent release of the TF by UBPs. TF is released and diffuses into the nucleus where it activates a set of reporter genes. The expression of these reporter genes serves as readout for the interaction.

transcription factor (TF) LexA-VP16 (bait) and a second protein of interest Y (or a cDNA library), which can either be transmembrane, membrane anchored or cytosolic to $N_{ub}G$ (prey). If an interaction between bait and prey occurs, C_{ub} and $N_{ub}G$ are forced into close proximity, resulting in the reconstitution of split-ubiquitin. The re-assembled protein is recognised by UBPs which subsequently cleave the polypeptide chain between C_{ub} and LexA-VP16. As a result, the artificial transcription factor is released from the membrane and translocates to the nucleus where it binds to the LexA operators situated upstream of a reporter gene via its LexA DNA binding domain. The VP16 transactivator domain then recruits the RNA polymerase II complex to the transcriptional start of the reporter gene, resulting in its transcriptional activation (Figure 2). The reporter genes used in the DUALmembrane system are two auxotrophic growth markers (HIS3 and ADE2), whose activation enables the yeast to grow on defined minimal medium lacking histidine or adenine, and lacZ, encoding the enzyme β-galactosidase. Consequently, the interaction between two proteins at the membrane of yeast is translated into a transcriptional readout, resulting in growth of yeast on selective medium and development of blue colouration in a β-galactosidase/X-Gal assay.

1.4 The SNARE complex protein syntaxin 5 (Stx5)

We discovered syntaxin 5 (Stx5) as a novel VLDL-R interactor (Figure 3). Stx5 is a ubiquitously expressed single-pass type IV membrane protein and belongs to the syntaxin family, a group of proteins which is mainly involved in the intracellular trafficking of vesicles by acting as soluble N-ethylmaleimide-sensitive factor-attachment protein receptors (SNAREs) (Jahn et al., 2003). The small, abundant and membrane-bound SNARE proteins are crucial mediators

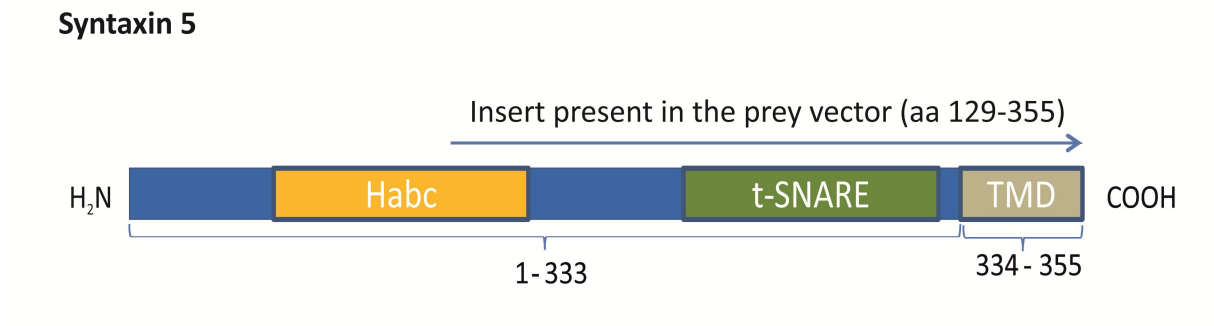

Figure 3 Schematic illustration of the Stx5 domain structure. Putative α-helices (yellow), t-SNARE motif (green) and transmembrane domain (TMD, grey) are indicated. The arrow displays the cDNA fragment of Stx5 present in the isolated prey vector pBT3N (aa 129-355).

of vesicle fusion in various vesicular transport processes along exocytic and endocytic pathways (Teng et al., 2001). Although, differing in structure and size all SNARE proteins share a similar coiled-coil segment in their cytosolic tail, termed a t-SNARE motif consisting of 60 – 70 amino acids which can bind to the SNARE motifs of other SNARE proteins like SNAP-25 and synaptobrevin to form the core SNARE complex. While Stx1, 2, 3 and 4 are resident in the plasma membrane where they administer exocytosis of intracellular vesicles (Bennett et al., 1993; Gaisano et al., 1996), Stx5 predominantly localises in the ER-Golgi intermediate compartment membranes and the *cis*-Golgi cisternae of the early secretory pathway (Dascher et al., 1994; Hay et al., 1998; Chao et al., 1999; Kasai and Akagawa, 2001). There are two ubiquitously expressed isoforms of Stx5 generated from one corporate messenger (m) RNA through alternative translational initiation (Hui et al., 1997), the 42 kDa/355 aa variant representing isoform 1 and the slightly shorter, 35 kDa/301 aa-large isoform 2 (herein referred to as Stx5S). The longer form primarily used in this study, and for convenience herein referred to as Stx5, carries an N-terminal extension motif, which is predicted to serve as ER retrieval signal, slightly keeping the protein within ER regions and

ER-Golgi intermediate compartments (ERGIC) (Hui et al., 1997). Still, like the shorter isoform Stx5S, Stx5 is exceedingly present in *cis*-Golgi stacks.

It has been proposed that Stx5 is involved in targeting and fusion of incoming carrier vesicles at three different sites: the fusion of vesicles derived from the ER with ER-Golgi intermediate compartment/vesicular tubular carriers (ERGIC/VTC), the formation of *cis*-Golgi stacks by assembling those ERGIC/VTCs and in the intra-Golgi fusion by the selective combination of a SNARE complex with other SNARE related proteins (Suga et al., 2005).

Beside Stx5's regulatory function in coat protein (COP) II vesicle transport there is evidence for its capability of directly interacting with several proteins, others than those of the SNARE complex machinery along their transport through ER to Golgi compartments. Representatively, it has been suggested that Stx5 binds and accumulates full-length presenilin (PS) in early secretory compartments and therefore affects the processing and trafficking of APP by modulating γ-secretase activity (Suga et al., 2004). Based on these findings we were interested whether this newly discovered interactor might be capable of modulating processing and/or trafficking of VLDL-R in a similar fashion.

1.5 Aims of the study

Concerning the described importance of intracellular adaptor proteins on the physiology of VLDL-R, we were interested in new binding partners and their potential impact on the receptor. We investigated the newly discovered interaction of Stx5 with VLDL-R *in vitro* and *in vivo.* Based on Stx5 binding we observed a specific trafficking and maturation phenotype of the VLDL-receptor. Therefore, we suggest a participation of Stx5 in bypassing the cell surface receptor around the classical secretory pathway directly to the cell surface, thereby regulating its expression levels, glycosylation stages and proteolytic cleavage.

2 MATERIAL AND METHODS

2.1 Antibodies

The monoclonal antibody 9E10 recognising the myc-epitope was generated from a mouse hybridoma cell line and used in a final dilution of 1:500 to detect the myc-tagged constructs after Western blotting (WB) and 1:50 for immunocytochemistry (IC) and immunoprecipitation (IP). Mouse anti-HA clone HA.11 (Covance) was used 1:5000 to visualise HA-tagged Stx5S. Endogenous VLDL-R was detected with rabbit polyclonal anti-VLDL-R (2897) recognising the C-terminus of VLDL-R (CPAISVVSTDDDLA) at a final dilution of 1:2000 after WB (kindly provided by Joachim Herz, UT Southwestern Medical Center, Dallas). For IC mouse monoclonal anti-VLDL-R (6A6) purchased from Santa Cruz Biotechnology, Inc (sc-18824) was used in a final dilution of 1:100. Stably expressed flag-tagged LRP1 mini-receptor domain IV (mLRP1 IV) was detected with mouse monoclonal anti-flag M2 (2 µg/ml; Sigma-Aldrich) in a final dilution of 1:2000. Detection of endogenously expressed LRP1 in HEK293T cells was carried out with rabbit polyclonal anti-LRP1 (1704) recognising the C-terminus of LRP1 at a final dilution of 1:10000 (Pietrzik et al., 2002). We generated a novel Stx5 polyclonal rabbit antibody recognising the first 15 N-terminal amino acids of Stx5 isoform 1 (MIPRKRYGSKNTDQC) conjugated to KLH for immunisation, performed by Genscript using standard protocols (Genscript, Piscataway, NJ, USA). Endogenous and transiently transfected human Stx5 was detected with this novel polyclonal anti-Stx5 (termed 2604) antibody. The antibody was used at a final dilution of 1:2000 for WB analysis or 1:200 for IC and IP. Monoclonal α-Tubulin antibody was obtained by Sigma-Aldrich and used at a final dilution of 1:5000 after WB. Normal rabbit IgG (sc2027) and normal mouse IgG (sc-2343) used as negative control for co-immunoprecipitation (Co-IP) were purchased

from Santa Cruz Biotechnology, Inc. Mouse anti-GM130 and mouse anti-PDI (both BD Bioscience) were used for IC in a final dilution of 1:200. For WB analysis anti-GM130 was used 1:2000. Rabbit anti-calnexin (Stressgen Bioreagents) was used in a final dilution of 1:2000 after WB (kindly provided by Jacqueline Trotter, University of Mainz, Germany). Mouse monoclonal anti-TGN46 clone 2F7.1 was used as *trans*-Golgi network (TGN) marker after WB in a final dilution of 1:1000 (ab2809, Abcam). Secondary HRP-conjugated goat antibodies against mouse and rabbit were purchased from Jackson Lab, Maine (USA) and used 1:5000 for WB. Mouse and rabbit AlexaFluor488 and AlexaFluor546 conjugated secondary antibodies (all Invitrogen) were used for visualising bound primary antibodies in IC studies in final dilutions of 1:500. Primary antibodies and corresponding dilutions used are listed in Table 1. Secondary antibodies and dilutions are presented in Table 2.

Antigen	Species	Dilution
anti-myc (9E10)	mouse/monoclonal	1:500 (WB); 1:50 (IP, IC)
Anti-HA (HA.11)	mouse/monoclonal	1:5000 (WB)
anti-VLDL-R (2897)	rabbit/polyclonal	1:2000 (WB)
anti-VLDL-R (6A6)	mouse/monoclonal	1:100 (IC)
anti-flag (M2)	mouse/monoclonal	1:2000 (WB)
anti-LRP1 (1704)	rabbit/polyclonal	1:10000 (WB)
anti-Stx5 (2604)	rabbit/polyclonal	1:2000 (WB); 1:200 (IP, IC)
α-Tubulin	mouse/monoclonal	1:5000 (WB)
anti-GM130	mouse/polyclonal	1:2000 (WB); 1:200 (IC)
anti-PDI	mouse/polyclonal	1:200 (IC)
anti-TGN46 (2F7.1)	mouse/monoclonal	1:1000 (WB)
anti-calnexin	rabbit/monoclonal	1:2000 (WB)

Table 1 Primary antibodies (WB: Western blot; IP: immunoprecipitation; IC: immunocytochemistry)

Antigen	Conjugate	Dilution
Goat-anti mouse IgG	HRP	1:5000 (WB)
Goat-anti rabbit IgG	HRP	1:5000 (WB)
Goat-anti mouse IgG	AlexaFluor488	1:500 (IC)
Goat-anti mouse IgG	AlexaFluor546	1:500 (IC)
Goat-anti rabbit IgG	AlexaFluor488	1:500 (IC)
Goat-anti rabbit IgG	AlexaFluor546	1:500 (IC)

Table 2 Secondary antibodies (WB: Western blot; IC: immunocytochemistry)

2.2 siRNA, cDNA constructs and cloning

pcDNA3.1Zeo encoding human VLDL-R was used as template to subclone VLDL-R with a 5' HindIII and 3' XbaI restriction site into pcDNA3.1A+mychis using the following fwd primer: 5'-CCCAAGCTTATGGGCACGTCCGCGCTCTG-3'; and rev primer: 5'-CCCTCTAGAAGCTAGATCATCA TCTGTGCT-3'. For the cloning of C-terminally myc-tagged VLDL-R NPVY→AAAA into pcDNA3.1A+mychis, VLDL-R was used as a template, and the mutation was introduced by an Overlap Extension PCR strategy, or four-oligo method (Lee et al., 2010), allowing selective introduction of base pair exchanges into DNA fragments. Two PCRs were performed separately using the following primer pairs: the outer fwd primer 5'-CCCAAGCTTATGGGCACGTCCGCGCTCTG-3' and the mutagenesis rev primer 5'-GTCCTCTTCAGTGGTTTTCAAGGCCGCCGCGGCGTCAAAGTTCATGCTTTTCAT-3'; the muta-genesis fwd primer 5'- ATGAAAAGCATGAACTTTGACGCCGCGGCGGCCTTGAAAACCACTGAAGA GGAC-3' and the outer rev primer 5'-CCCTCTAGAAGCTAGATCATCATCTGTGCT-3'. Two products resulted from these PCRs overlapping in the middle and both containing the respective mutation. To gain the full-length VLDL-R construct deprising the desired NPVY→AAAA exchange, a third PCR was run using the two mutagenesis fragments as

template and the outer primers. Human Stx5 isoform 1 (referred to as Stx5) cDNA (Accession number: NM_003164) in pCMV6-XL5 was obtained from OriGene Technologies Inc. (Rockville), and HA-tagged isoform 2 (referred to as Stx5S) in pcDNA3 was kindly provided by Kei Suga (Kyorin University School of Medicine, Tokyo, Japan). Stx5 knock-down was performed with esiRNA purchased from Sigma-Aldrich targeting the following 5'-region of the open reading frame of Stx5: 5'- GAACACGGATCAGGGTGTCTACCTGGGTCTCTCAAAGACAC AGGTCCTGTCCCCTGCAACTGCTGGCAGTAGCAGCAGCGACATCGCCCCTCTGCCCCCCCCAGTGAC CCTCGTCCCTCCCCCTCCCGACACCATGTCCTGCCGGGATCGGACCCAGGAGTTTCTGTCTGCCTGCA AGTCGCTGCAGACCCGTCAGAATGGAATCCAGACAAATAAGCCAGCTTTGCGTGCTGTCCGACAACG CAGTGAATTCAC-3'. Non-targeting, scrambled siRNA obtained from Sigma-Aldrich served as negative control.

For the split-ubiquitin based cDNA library screening approaches and re-transformation experiments pcDNA3.1Zeo encoding human VLDL-R was used as template to subclone VLDL-R into the yeast - E. coli shuttle type-I bait vector pCCW-SUC (DualSystemsBiotech). The VLDL-R specific N-terminal signal sequence (aa 1-81) was omitted by using the following fwd primer: 5'-CTTTTCCTTTTGGCTGGTTTTGCAGCCAAAATATCTGCAATGGGGAGAAAAGCCAAATG TGA-3'. Between the C-terminus of VLDL-R and the reporter module C_{ub}-LexA-VP16 a 7 aa-linker was added by using the rev primer: 5'-GTTGATCTGGAGGGATCCCCCCCGACATGGTCG ACGGTATAGCTAGATCATCATCTGTGC-3'. A truncated form of LRP1 (aa 3531-4543) containing the 85 kDa subunit and part of the α-chain was subcloned into pCCW-SUC with the fwd primer: 5'-CTTTTCCTTTTGGCTGGTTTTGCAGCCAAAATATCTGCAATGTCTGAGTACCAGGTCCT GTA-3' and rev primer: 5'- GTTGATCTGGAGGGATCCCCCCCGACATGGTCGACGGTATTGCCA AGGGGTCCCCTATCTC-3' including a 7aa-linker between the C-terminus of LRP1 and C_{ub}-LexA-VP16. Myc-tagged mouse Dab1 (isoform Dab555) in pCDNA3.1Zeo+ was kindly

provided by Uwe Beffert (Boston University, MA, USA) and was subcloned into the prey vector pDSLNx (DualSystemsBiotech) fusing the positive control protein to the C-terminus of the $N_{ub}G$ cassette using the following fwd primer: 5'- GGATCCAAGCAGTGGTATCAACGCAGAG TGGCCATTACGATGTCAACTGAGACAGAACT-3' and rev primer: 5'-GTGACATAACTAATTACATG ACTCG AGGTCGACGGTATCCTAGCTACCGTCTTGTGGAC-3'.

For GST pull-down experiments the cytosolic domain of human VLDL-R (aa 820-873) following a C-terminally positioned myc-tag, was fused C-terminally to GST by subcloning into pGEX-2T (GE Healthcare) using the fwd primer: 5'- CGGGATCCAGGAATTGGCAACATAA-3' and rev primer: 5'-GGAATTCTCACAGATCCTCTTCTGAGATGAGTTTTTGTTCAGCCAGATCATCATC TGTGCTTACAACTGATA-3'. A truncated form of LRP1 (aa 4445-4544) consisting of the cytosolic domain of the receptor was subcloned into pGEX-2T using the following fwd primer: 5'-CGGGATCCAAGCGGCGAGTCCAAGGGGCTA-3' and rev primer: 5'-AAGCTTCTATGCCAAGGGGTCCCCTAT-3'. In order to make stable LRP1 deficient CHO cells (13-5-1) overexpressing human LRP1, a LRP1 construct consisting of the 85 kDa subunit and a truncated extracellular domain (ligand-binding domain IV) with an N-terminally fused flag-tag was cloned into pLBCX.

2.3 cDNA library screen in yeast (mbSUS) and plasmid isolation

The cDNA library screen was performed according the manufacturer's instructions (DualSystemsBiotech). Briefly, the yeast strain NMY.32 (DualSystemsBiotech) expressing the bait construct VLDL-R-C_{ub} was brought to a fluid-colony OD_{600} of 0.6 – 0.7 and transformed with 28 µg human cDNA library (DualSystemsBiotech) using the *LiAc*/SS carrier DNA/PEG method (Ito et al., 1983). Subsequently, full medium-recovered yeast was plated out on prepared selective plates lacking the interaction reporter adenine (SD -L/-W/-Ade) and

incubated on 30°C for 3-4 days. Afterwards, grown colonies were picked and rescued on selective plates prior to plasmid isolation. Therefore, cell pellets from overnight cultures of the according yeast were incubated each with 5 units/µl H_2O lyticase (Sigma-Aldrich) for 1 h and, subsequently mixed with SDS in a final concentration of 4 %. Extracts of the plasmid mixtures were further prepared using the plasmid isolation kit NucleoSpin (Macherey-Nagel) according to the manufacturer's instructions. To separate the isolated plasmids (pCCW-SUC and pBT3N), extracts were re-transformed into the *E. coli* strain XL1-blue and plated out on ampicillin containing LB-plates, which resulted in the selective growth of pBT3N carrying bacteria (pCCW-SUC: kanamycin resistance; pBT3N: ampicillin resistance). Isolated plasmids were used for further re-transformation experiments in yeast.

2.4 Re-transformation of potential targets in yeast and *β*-galactosidase assay

For *in vivo* validation of protein interaction in the yeast strain NMY.32, respective prey vectors were re-transformed into bait bearing yeast, the *LiAc*/SS carrier DNA/PEG method was used according to manufacturer's instructions. Transformation mixtures were plated out on non-selective plates lacking the auxotrophic markers for plasmid uptake leucine and tryptophan (SD -L/-W), and selective plates (SD -L/-W/-Ade), respectively and grown for three days prior to analysis by growth. Growth on SD -L/-W plates indicated presence of both bait and prey vector and therefore, successful uptake of a prey plasmid by the bait expressing yeast, since the genes encoding an enzyme crucial for the production of leucine or tryptophan are positioned on the respective expression vectors (pCCW-SUC: leu2; pBT3-N: trp1). To screen for the activity of the LacZ reporter encoding for *β*-galactosidase transformation mixtures were dispersed on selective plates comprising 40 µg/ml of X-Gal (DualSystemsBiotech) and grown for 2 days. Presence of indigo dye, originated from a

cleaving product of X-Gal by *β*-galactosidase worked as further readout for an interaction between bait and prey.

2.5 Cell culture and drug treatment

HEK293T cells were cultured in Dulbecco's Modified Eagle Medium (DMEM) supplemented with 10 % fetal bovine serum, 1 mM sodium pyruvate, 100 units/ml penicillin and 100 µg/ml streptomycin (all from Invitrogen). Transient transfection of HEK293T cells (2 µg cDNA/6-Well) was performed for 24 to 48 h using the calcium phosphate-mediated transfection method. 48 h-transfection of siRNA was carried out using X-tremeGENE siRNA Transfection Reagent (Roche) according to manufacturer's instructions. LRP1-deficient CHO cells (13-5-1) stably overexpressing flag-tagged mLRP1 IV were grown in Alpha Minimum Essential Medium (α-MEM; Lonza) supplemented with 10 % fetal bovine serum, 1 mM sodium pyruvate, 100 µg/ml penicillin and 100 µg/ml streptomycin. Liver derived Hep-G2 cells were purchased from CLS cell Lines Service GmbH (Eppelheim, Germany) and were cultured in DMEM Ham's F12 (Invitrogen) supplemented with 10 % fetal bovine serum, 1 mM sodium pyruvate, 100 µg/ml penicillin, 100 µg/ml streptomycin and 2 mM L-glutamine. Primary cortical neurons were isolated from mouse embryos (BL6/J wild-type) at embryonic day 16 and cultured in Neurobasal medium containing B-27 supplement and 1xGlutaMAX (both Invitrogen). All cell types were maintained in a humified incubator at 37 °C and 5 % CO_2.

To inhibit proteasomal degradation of VLDL-R prior to a pulse-chase experiment, HEK293T were treated with 50 µM MG132 (Merck Millipore, Darmstadt) for 4 h. Lysosomal degradation in HEK293T cells was blocked by 10 mM NH_4Cl (Roth, Karlsruhe) for 12 h respectively. To inhibit anterograde transport through secretory compartments, cells were treated with 10 µg/ml fungal metabolite brefeldin A (BFA, Sigma; B-7651) for 4 h.

2.6 SDS-PAGE and Western blotting

Cells were washed with ice-cold PBS, scraped off culture dishes and lysed in NP-40 lysis buffer (500 mM Tris pH 7.4, 150 mM NaCl, 5 mM EDTA, 1 % Nonidet P-40, 0.02 % sodium azide), plus complete protease inhibitors (Roche). Debris was pelleted by centrifugation at 16.000 x *g* for 20 min at 4 °C in a microcentrifuge. Equal amounts of total protein (20 µg), determined by BCA protein assay (Pierce Chemicals) were used for lysate analysis. Samples were incubated with SDS sample loading buffer (0.625 M Tris-HCl, pH 6.8, 2 % w/v SDS, 10 % w/v glycerol, 5 % *ß*-mercaptoethanol) and heat denatured for 5 min. Proteins were either electrophoresed on 4-12 % NuPage (Novex®, Invitrogen) gradient gels or 10 % tris-glycine gels (BioRad) and transferred onto nitrocellulose membranes (Millipore). Non-specific binding to membranes was blocked with 5 % non-fat dry milk in TBS containing 0.01 % Tween-20 (Roth) for 1 h, before incubation with the approximate primary and secondary antibodies. Proteins were detected using enhanced chemiluminescence (Millipore) by using the LAS-3000mini (Fujifilm).

2.7 Co-immunoprecipitation

Prior to IP, HEK293T cells were transiently co-transfected with human myc-tagged VLDL-R in pcDNA3.1A+mychis and human Stx5 in pCMV6-XL5 for 24 h. Cell lysates were prepared using NP-40 plus protease inhibitors (Roche). VLDL-R (100 µg of total proteins) was immunoprecipitated from HEK293T lysates with monoclonal antibody 9E10 binding the myc-epitope in the presence of Protein A agarose beads (Invitrogen) at 4 °C overnight. Beads were collected carefully by low speed centrifugation and washed three times with ice-cold NP-40 lysis buffer before proteins were recovered by boiling in 2x SDS sample buffer for 5

min. Samples were separated on 10 % tris-glycine gels prior to WB onto nitrocellulose membranes. Co-immunoprecipitated Stx5 was detected with 2604.

For reverse Co-IP, HEK293T cells were either co-transfected with myc-tagged VLDL-R in pcDNA3.1A+mychis and human Stx5 in pCMV6-XL5 or VLDL-R alone for 24 h. Stx5 (100 µg of total proteins) was immunoprecipitated from lysates with rabbit polyclonal anti-Stx5 (2604) in the presence of Protein A agarose beads at 4 °C overnight. All further steps were carried out as described above. Co-immunoprecipitated VLDL-R was detected with 9E10.

For Co-IP of endogenous VLDL-R and Stx5, lysates from cortical neurons were prepared and Stx5 (100 µg of total proteins) was immunoprecipitated using 2604. Further steps were carried out as described above. Co-immunoprecipitated VLDL-R was detected on WB using 2897 anti-VLDL-R antibody.

2.8 GST protein purification and pull-down

For purification of GST fusion proteins, respective plasmids were transformed into BL21 (Agilent Technologies) and expression was induced by Isopropyl-*β*-D-thiogalactopyranosid (IPTG) for 4 h. Proteins were recovered by sonication and subsequent Triton X-100 (Sigma) lysis overnight. Proteins were purified using glutathione-agarose beads (Sigma-Aldrich) and protein concentration was determined on a 10 % tris-glycine gel with BSA standards (0.5-5 µg) followed by coomassie staining. Prior to GST pull-down, HEK293T cells were transiently transfected with human Stx5 in pCMV6-XL5 and grown on 100 mm dishes to 90 % confluency. Cell lysates were prepared using NP-40 buffer plus protease inhibitors and incubated with 10 µg of respective GST fusion proteins overnight. Afterwards, samples were incubated with 40 µl gluthatione-agarose beads for 4 h under rotation at 4 °C and, subsequently washed two times with CHAPS lysis buffer (50 mM Tris-Cl pH 7.5, 150 mM

NaCl, 0.02 % NaN_3, 0.5 % CHAPS) before protein were recovered by boiling in 2x SDS sample buffer for 5 min. Prior to WB samples were separated on 10 % tris-glycine gels. Pulled-down Stx5 was visualised using 2604.

2.9 Immunofluorescence and confocal microscopy

HEK293T and Hep-G2 cells were grown on poly-L-ornithine (Sigma-Aldrich) coated coverslips (Marienfeld) in 6-well plates (TPP). HEK293T cells were transiently transfected (calcium phosphate-mediated transfection method) with pcDNA3.1A+mychis VLDL-R and pCMV6-XL5 Stx5 for 24 h. Subsequently, cells were washed three times with PBS at 37 °C and fixed with 4 % paraformaldehyde at room temperature for 10 min. After three washing steps with PBS, cells were blocked in 2 % (w/v) bovine serum albumin in PBS plus 4 % (v/v) Triton X-100 (both from Sigma-Aldrich) for 30 min. Incubation with primary antibodies against myc-tagged VLDL-R (9E10), endogenous VLDL-R (2897, 6A6), Stx5 (2604), the ER marker PDI and the *cis*-Golgi matrix protein GM130 was carried out overnight at 4 °C in blocking solution. After three washing steps in PBS, cells were incubated with AlexaFluor488 and AlexaFluor546 conjugated secondary antibody (Invitrogen) at RT for 1 h. Nuclei were counterstained with 5 µM DRAQ5 (Biostatus Limited) in PBS for 10 min. After three washing steps in PBS, coverslips were mounted with ProLong Gold antifade reagent (Invitrogen). Images were acquired with a LSM710 confocal laser scanning microscope using ZEN 2008 software (Carl Zeiss).

2.10 PNGaseF/Endoglycosidase H (EndoH) mediated removal of carbohydrate residues from VLDL-R

HEK293T cells were either co-transfected with human myc-tagged VLDL-R in pcDNA3.1A+mychis and human Stx5 in pCMV6-XL5 or transfected with VLDL-R respectively. PNGaseF and Endoglycosidase H (EndoH, both from New England BioLabs) digestion of VLDL-R was performed according to the manufacturer's instructions. Briefly, 20 µg of the respective lysates were denatured with 1x glycoprotein denaturing buffer at 95 °C for 10 min. After the addition of 1/10 volume of 10x reaction buffer either 2 µl PNGaseF plus 1/10 volume of NP40, 2 µl of EndoH or 2 µl H_2O as digestion control were added to the appropriate samples. Afterwards, reaction mixes were incubated at 37 °C for 1 h. In the following, the reaction products were separated on 4-12 % NuPage gradient gels and analysed by WB.

2.11 Metabolic labeling and immunoprecipitation of VLDL-R

HEK293T cells either transiently co-transfected with human myc-tagged VLDL-R in pcDNA3.1A+mychis and human Stx5 in pCMV6-XL5 or transfected with VLDL-R alone were plated in 6-well culture dishes. After 24 h, the cultures were pulse-labeled for 15 min at 37 °C with 1 ml methionine-free DMEM containing 150 µCi of [^{35}S] methionine/cysteine (EasyTag™ EXPRESS^{35}S Protein Labeling Mix). Cells were lysed immediately after the pulse (time 0), or chased for 6-72 h to determine the maturation of VLDL-R. Cell pellets were lysed in 500 µl of NP-40 lysis buffer plus protease inhibitors, and lysates were cleared by centrifugation at 16.000 x *g* for 20 min. Post-nuclear supernatants were incubated at 4 °C with 9E10 and protein A agarose beads overnight. Immunocomplexes were washed twice

with NP-40 buffer, one time with PBS, and eluted from the beads by boiling in 30 µl of 2x SDS sample buffer for 10 min. Proteins were separated on 4-12 % NuPage gradient gels followed by autoradiography on an X-ray film at -80 °C for a minimum of 12 h.

2.12 Cell surface-biotinylation

HEK293T cells were either transiently co-transfected with human myc-tagged VLDL-R in pcDNA3.1A+mychis and human Stx5 in pCMV6-XL5 or transfected with VLDL-R respectively and grown on 60-mm dishes to 90 % confluency. After three washing steps with ice-cold PBS, cell surface proteins were biotinylated with 0.5 mg/ml Sulfo-NHS-LC-LC-Biotin (Pierce) in ice-cold PBS at 4 °C for 40 min. The biotin solution was exchanged once after 20 min. Cells were washed four times with ice-cold PBS containing 50 mM NH_4Cl to quench unconjugated biotin and lysed in NP-40 buffer. Equal amounts of proteins were incubated with NeutrAvidin agarose resin (Pierce) at 4 °C overnight. Biotinylated proteins were recovered by boiling in 2x SDS sample buffer for 5 min and separated on 4-12 % NuPage. To examine surface levels of VLDL-R in cells suffered from low temperature, HEK293T cells were transiently transfected with either myc-tagged VLDL-R in pCDNA3.1A+ with or without Stx5 in pCMV6-XL5 for 24 h and cultured at 15°C for indicated time points (h). Further steps were carried out as described above.

2.13 Subcellular fractionation by a continuous iodixanol gradient

To investigate intracellular localisation of VLDL-R with either high or moderate expression levels of Stx5, HEK293T cells were transiently co-transfected with myc-tagged VLDL-R and Stx5 or transfected with VLDL-R alone and grown to 100 % confluency on 10 cm culture-

dishes. Subsequently, cells were washed with ice-cold PBS and collected in homogenisation medium (HM), consisting of 0.25 M sucrose, 1 mM EDTA and 10 mM Hepes-NaOH with pH of 7.4. Cells were broken by 10 - 15 passages through a syringe connected to a 25-gauge needle (Braun), followed by a centrifugation step at 1200 x *g* for 20 min to dispose of the nuclear fraction. Accordingly, pellets were discarded and post-nuclear supernatants layered upon continuous 5-25 % iodixanol gradients prepared with OptiPrep™ (Sigma-Aldrich) and formed by diffusion of discontinuous gradients according to the manufacturer's instructions. Subsequent to centrifugation at 138.000 x *g* for 3 h in a *L8-60M* ultracentrifuge of Beckman using the swing-out rotor SW40Ti, fourteen 900 µl-fractions were collected from the top of each gradient. For WB analysis, 30 µl of each fraction were loaded on 10 % tris-glycine gels and defined by using organelle specific antibodies. To ensure comparability of the respective fractions from Stx5 overexpressing and endogenously expressing cells, percentage of distributed iodixanol in each fraction was measured using an automatic master refractometer from ATAGO.

2.14 Quantification and statistical analysis

Western blots were quantified by densitometry using ImageJ 1.44. All graphs and statistical analyses were prepared using GraphPad Prism 4 software (GraphPad). Data were analysed by two-way analysis of variance (ANOVA) coupled to Bonferroni post hoc test or *t* test. $p < 0.05$ was considered as statistically significant.

3 RESULTS

3.1 The human brain cDNA library screen revealed Stx5 as potential interactor of VLDL-R

To identify novel interaction partners of the VLDL-receptor we performed a membrane-based split-ubiquitin cDNA library screening approach in yeast using a human brain library and determined a huge amount of potential targets with diverse biological functions. By re-transformation of the isolated fragments into the bait expressing yeast we were able to exclude false-positive interactions and limited the scope of evident targets to those listed in Table 3. Indicated are genetic description of the interactors, the amount of independent clones found and the various biological processes the respective proteins partake.

Interactors identified	Number of clones	Biological processes involved
ARL6IP5	12	L-glutamate transport
CHN1	3	intracellular signal transduction
ATP6V0D1	2	ATP hydrolysis coupled proton transport
PEX5L	2	protein targeting
RAB5C	2	protein transport
ARFGEF2	2	regulation of ARF protein signal transduction
RTN4	2	neurogenesis
GLUL	2	cell proliferation
MORF4L2	2	transcription regulation
BCAP31	2	protein transport, apoptosis
SACM1L	2	phosphatidylinositol dephosphorylation
SOX9	2	transcription regulation
STX5	1	ER to Golgi vesicle-mediated transport
AGT	1	acetyltransferase activator activity
ROPN1B	1	signal transduction
DBNDD2	1	negative regulation of protein kinase activity
PSPC1	1	transcription regulation

GPM6B	1	protein transport, neurogenesis
YIF1A	1	protein transport
HMOX1	1	heme oxidation
KNDC1	1	signal transduction
CRIPAK	1	regulation of cytoskeleton organisation
ERCC2	1	transcription regulation
ITM2A	1	unknown
SIRT2	1	mitosis
RHEB	1	positive regulation of TOR signaling cascade
ND4	1	transport
ATP6AP2	1	regulation of MAPK cascade
TF	1	ion transport
SERINC1	1	lipid biosynthesis
SLC6A8	1	ion transport
CCNH	1	transcription regulation
COX1	1	lipid biosynthesis
CCKBR	1	cell proliferation
KDR	1	angiogenesis, differentiation
MKL1	1	transcription regulation

Table 3 Potential interactors with VLDL-R found in a membrane-based YTH screen. The table shows potential interactors with the cytoplasmic domain of VLDL-R from a membrane-based YTH screen after re-transformation procedure for exclusion of false-positive interactions. Target names, number of identified clones and approximate function of the particular proteins are presented.

3.2 Re-transformation of Stx5 in bait expressing yeast revealed specific *in vivo* interaction with VLDL-R

As a matter of course, we were not able to study all targets in detail. One interesting target we chose for further analysis is the ubiquitously expressed type IV transmembrane protein Stx5 (Figure 3). To assure true interaction of Stx5 and VLDL-R *in vivo* we performed re-transformation of the isolated Stx5 fragment (aa 129 – 355) into bait expressing yeast

(NMY.32 VLDL-R-C_{ub}) and additionally included yeast expressing a truncated C_{ub}-fused LRP1 construct (NMY32 LRP1β-chain-C_{ub}) as negative control for VLDL-R specific binding of Stx5 (Figure 4). Re-transformation of NMY.32 VLDL-R-C_{ub} and NMY.32 LRP1β-chain-C_{ub} with Dab1, a well characterised interactor of VLDL-R and LRP1 (Trommsdorff et al., 1998; Trommsdorff et al., 1999) served as positive control for proper function of the C_{ub}-LexA-VP16 fused bait constructs, whereas the empty control vector pDSLN was transformed as negative control to define possible background growth resulting e.g. from bait self-activation. All re-transformed

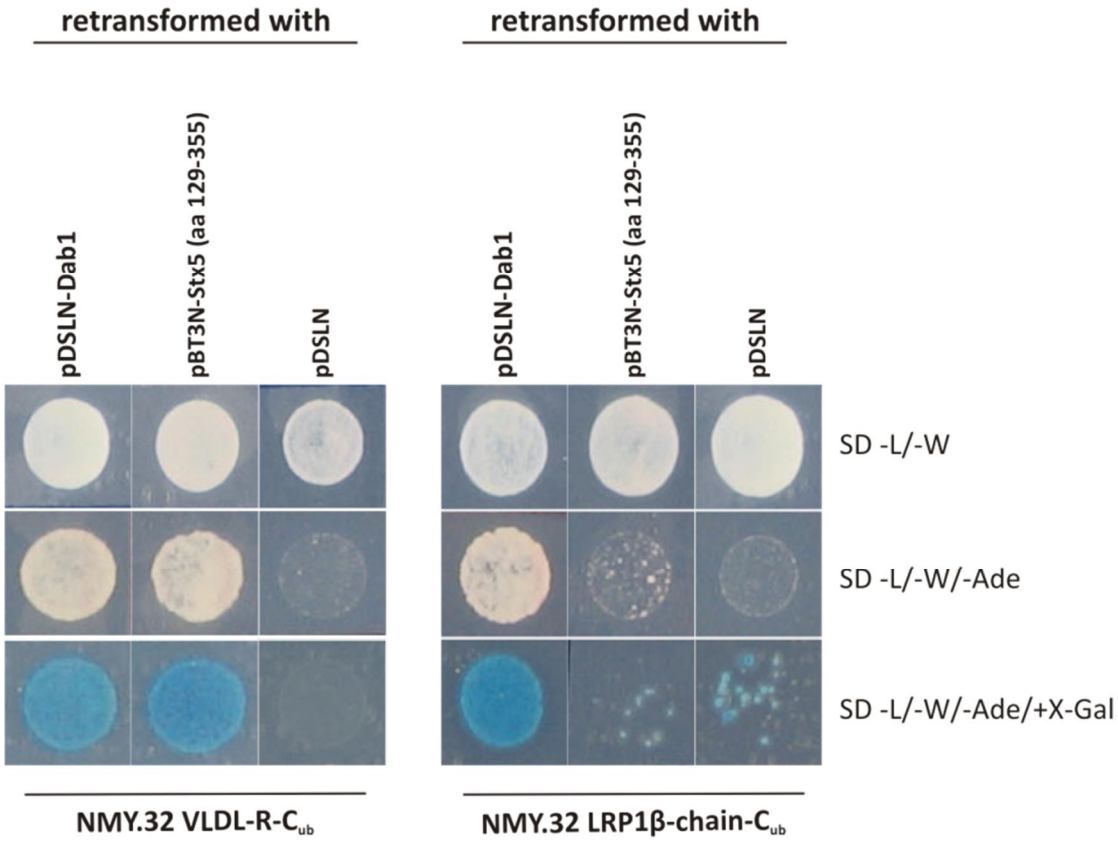

Figure 4 Re-transformation of pBT3N-Stx5 (aa 129-355) into the bait expressing yeast strain NMY.32 to exclude Stx5 as false positive interactor *in vivo*. NMY.32 yeast expressing either VLDL-R-C_{ub} (*left block*) or LRP1β-chain-C_{ub} (*right block*) was each re-transformed with the isolated pBT3N-Stx5 (*middle panel*), with pDSLN-Dab1 serving as positive control (*left panel*) or the empty vector pDSLN (*right panel*) serving as negative control. Mixtures were plated on non-selective (SD -L/-W) and selective plates either lacking (SD -L/-W/-Ade) or containing X-Gal (SD -L/-W/-Ade/+X-Gal). Growth of yeast on SD -L/-W/-Ade together with strong blue coloration on SD -L/-W/-Ade/+X-Gal served as readout for a positive interaction of the prey proteins with the respective bait.

yeast properly grew on non-selective SD -L/-W plates indicating effective uptake of the respective N_{ub}-vectors. Re-transformation of the VLDL-R or LRP1 expressing strain with pDSLN-Dab1 resulted in both, growth of the respective yeast on selective plates (SD -L/-W/-Ade) and a strong blue colouration on plates with additive X-Gal (SD -L/-W/-Ade/+X-Gal), pointing to strong interaction of Dab1 with both receptors and thus, functionality of the bait constructs. However, yeast re-transformed with the empty control vector pDSLN did not exceed slight background growth. NMY.32 VLDL-R-C_{ub} co-expressing the Stx5 fragment grew properly on selective plates and addition of X-Gal revealed blue colouration. In contrast, Stx5 re-transformed NMY.32 LRP1β-chain-C_{ub} was not able to grow significantly as defined by comparison to background growth of pDSLN transformed yeast expressing N_{ub}G lacking any fusion protein. Taken together, the re-transformation assay excluded false-positive interaction of VLDL-R and Stx5 in yeast and moreover, suggested a specific binding of Stx5 to the cytosolic domain of VLDL-R *in vivo,* since there was no positive readout when expressed with LRP1.

3.3 *In vitro* validation of the interaction between VLDL-R and Stx5 by co-immunoprecipitation and GST pull-down experiments

To confirm the established *in vivo* interaction of VLDL-R and Stx5 observed in yeast, we performed *in vitro* Co-IP studies (Figure 5). Therefore, HEK293T cells were transiently co-transfected using myc-tagged VLDL-R and Stx5 and subjected to Co-IP analysis (Figure 5A, *left and middle panel*). These experiments verified that Stx5 could be successfully co-immunoprecipitated with VLDL-R (Figure 5A, *left panel*) and vice versa (Figure 5A, *middle panel*). To exclude overexpression artefacts we set out to analyse whether endogenous

expression levels of Stx5 would be sufficient to co-precipitate VLDL-R. Therefore, cells expressing exogenous VLDL-R and endogenous Stx5 were subjected to Co-IP using anti-Stx5 antibody 2604, recognising endogenous Stx5. Although, the detected amounts of co-

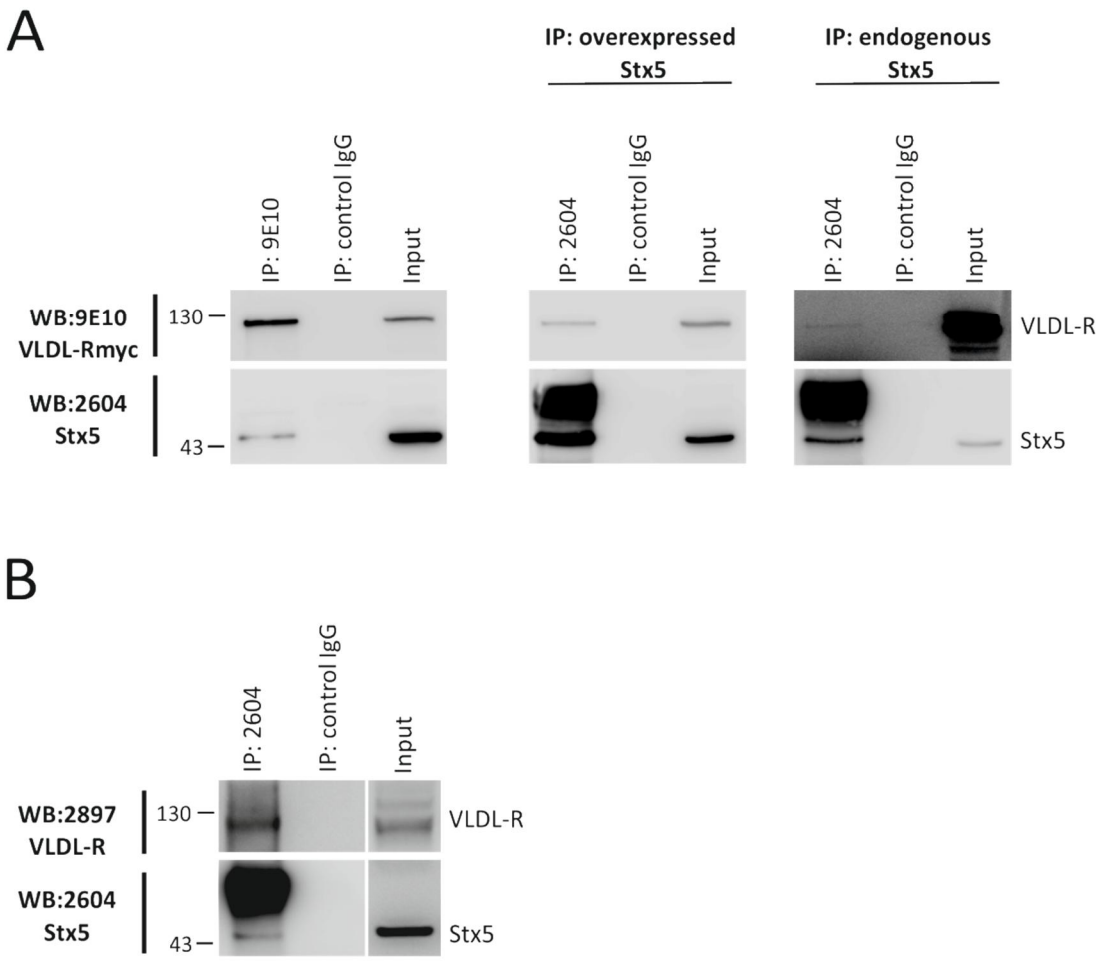

Figure 5 Co-immunoprecipitation of VLDL-R and Stx5. HEK293T cells were transiently co-transfected with myc-tagged VLDL-R in pcDNA3.1A+ and Stx5 pCMV6-XL5 (A, *left and middle panel*) or transfected with VLDL-R alone for co-immunoprecipitation (Co-IP) of VLDL-R with endogenous Stx5 (A, *right panel*). For immunoprecipitation (IP) of endogenous proteins (B) lysates from primary cortical neurons derived from BL6/J wild-type mice at DIV 14 were used. VLDL-R was immunoprecipitated with 9E10 antibody. Co-immunoprecipitated Stx5 was detected after Western blotting using anti-Stx5 antibody 2604. Mouse IgG antibody was used as negative control for IP. Stx5 was immunoprecipitated using anti-Stx5 antibody 2604. Co-immunoprecipitated VLDL-R was detected after Western blot using 9E10. Rabbit IgG antibody served as negative control for IP.

immunoprecipitated VLDL-R were lower as under Stx5-overexpressing conditions, we could still demonstrate binding of endogenous Stx5 to VLDL-R (Figure 5A, *right panel*). To examine the interaction of both endogenous VLDL-R and Stx5, we prepared lysates from primary cortical neurons derived from BL6/J wild-type mice. IP with anti-Stx5 antibody 2604 resulted in appropriate amounts of co-immunoprecipitated VLDL-R (Figure 5B). These results indicated a native interaction of VLDL-R and Stx5, or at least, let us omit artificial binding due to overexpression of one or both proteins.

Next, we addressed the question whether this interaction was due to potential co-purification of a common membrane fraction in the IP experiments, or to actual interaction of the cytosolic domains of both proteins. Therefore, GST pull-down experiments were performed using the C-terminal domains of VLDL-R and LRP1 exclusive of the receptors' transmembrane domains fused to GST as baits (Figure 6). Since Stx5 had not revealed any binding property with LRP1 in previously performed re-transformation experiments, we used

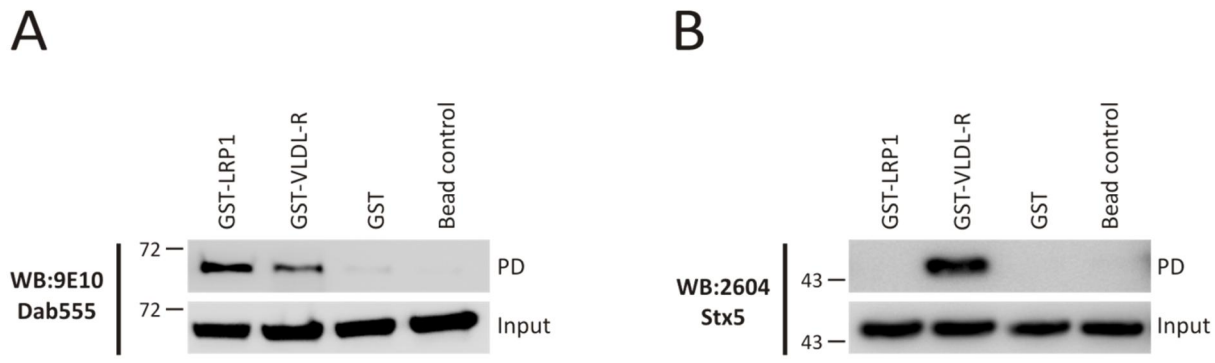

Figure 6 GST pull-down of Dab1 and Stx5 with GST fusion proteins. Lysates of Dab1 (Dab555) (A) or Stx5 (B) transfected HEK293T cells were incubated with GST fusion proteins of VLDL-R and LRP1, GST or gluthatione-agarose beads alone. Pulled-down proteins were detected after Western blotting using 9E10 against myc-tagged Dab555 (A) or anti-Stx5 antibody 2604 (B). (A) Interaction of GST-LRP1 and GST-VLDL-R with the positive control Dab555 revealed functionality of both constructs. (B) Stx5 was specifically precipitated with GST-VLDL-R.

GST-LRP1 as negative control for specific binding of Stx5. Prior to the approach, we determined the functionality of our GST fusion proteins by incubation with lysates of HEK293T cells overexpressing myc-tagged Dab1 (isoform Dab555), known to bind to VLDL-R and LRP1. As expected, both GST-VLDL-R and GST-LRP1 were capable of precipitating the positive control protein Dab1 (Figure 6A).

For the actual pull-down experiment with Stx5, HEK293T cells were transiently transfected with the particular construct. Prepared lysates were then incubated with 10 µg of the fusion protein GST-VLDL-R (Figure 6B, *lane 2*), whereas incubation with GST-LRP1 (Figure 6B, *lane 1),* GST alone (Figure 6B, *lane 3*) and beads (Figure 6B, *lane 4*) served as negative controls. Exclusively in lysates incubated with GST-VLDL-R we were able to detect precipitated Stx5, defining specific binding of Stx5 to the C-terminus of VLDL-R.

3.4 VLDL-R and Stx5 co-localise in perinuclear vesicles representing early secretory compartments

To analyse the localisation of this interaction, we performed co-immunostaining studies in HEK293T expressing VLDL-R and Stx5. Co-staining of VLDL-R together with anti-PDI or anti-GM130 antibodies revealed localisation of the transiently expressed receptor both, in ER compartments and *cis*-Golgi cisternae (Figure 7A and B, *Merge, arrowheads*). Since it had been shown previously that Stx5 is localised both in ER and *cis*-Golgi compartments we used PDI and GM130 to confirm the localisation of transfected Stx5 within ER and *cis*-Golgi (Figure 8A and B, *Merge, arrowheads*). By comparison of the *cis*-Golgi structure (Figure 8B, *GM130*) in cells expressing high and low amounts of Stx5 (Figure 8B, *Stx5*), we found that Stx5 overexpression did not lead to considerable Golgi fragmentation, which had been previously

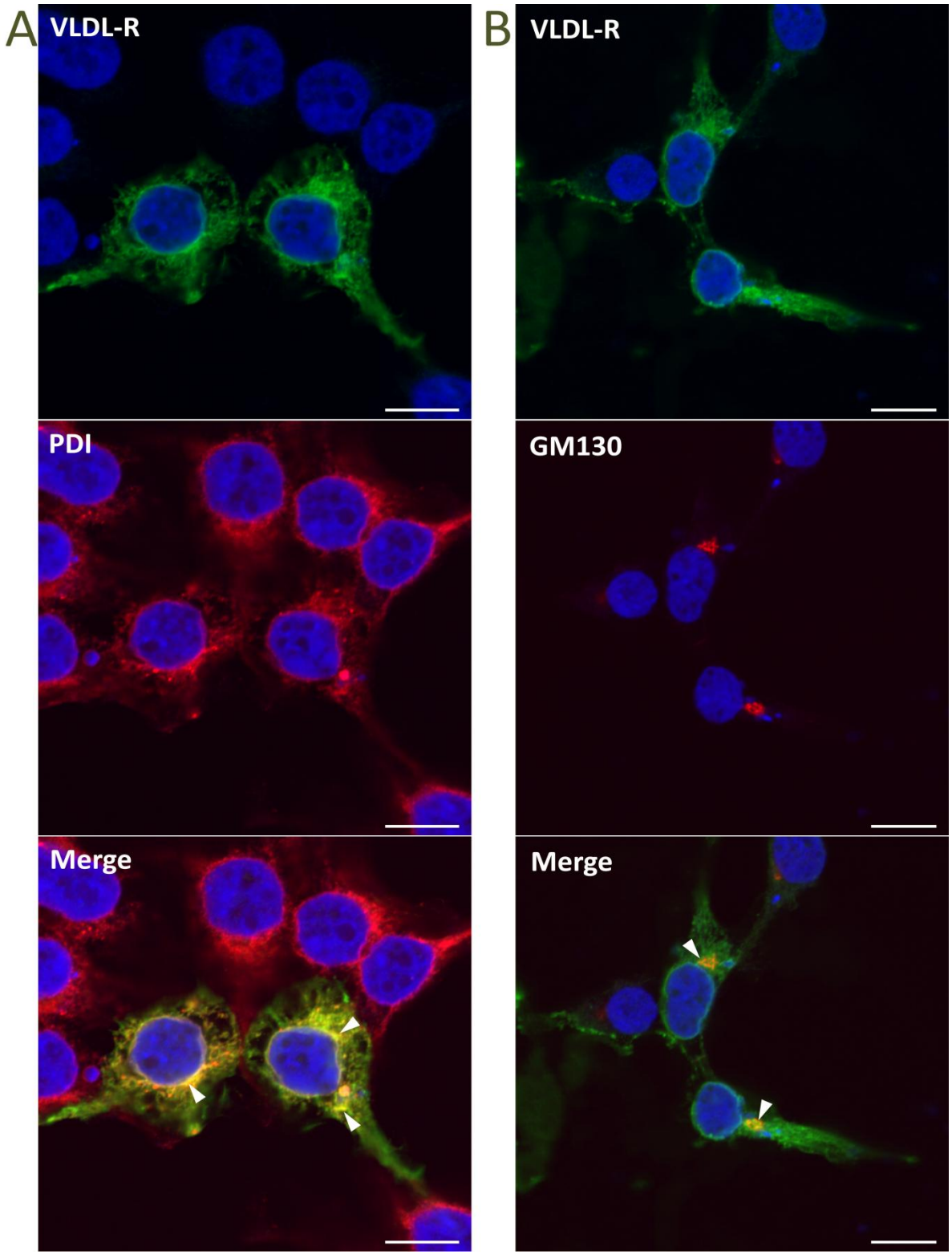

Figure 7 Co-immunostainings of VLDL-R with ER marker PDI and *cis*-Golgi marker GM130. HEK293T cells were transiently transfected with VLDL-R in pCDNA3.1Zeo, fixed in paraformaldehyde and co-immunostained with rabbit anti-VLDL-R antibody 2897 and mouse anti-PDI (A) or mouse anti-GM130 (B), followed by incubation with respective AlexaFluor488 and AlexaFluor546 conjugated secondary antibodies. The green fluorescence represents VLDL-R (A and B), red fluorescence PDI (A) or GM130 (B). Nuclei were counterstained using DRAQ5 (*blue*). Co-stainings revealed localisation of VLDL-R in ER and *cis*-Golgi compartments (A and B, *Merge, arrowheads*). Scale bar = 10 µm.

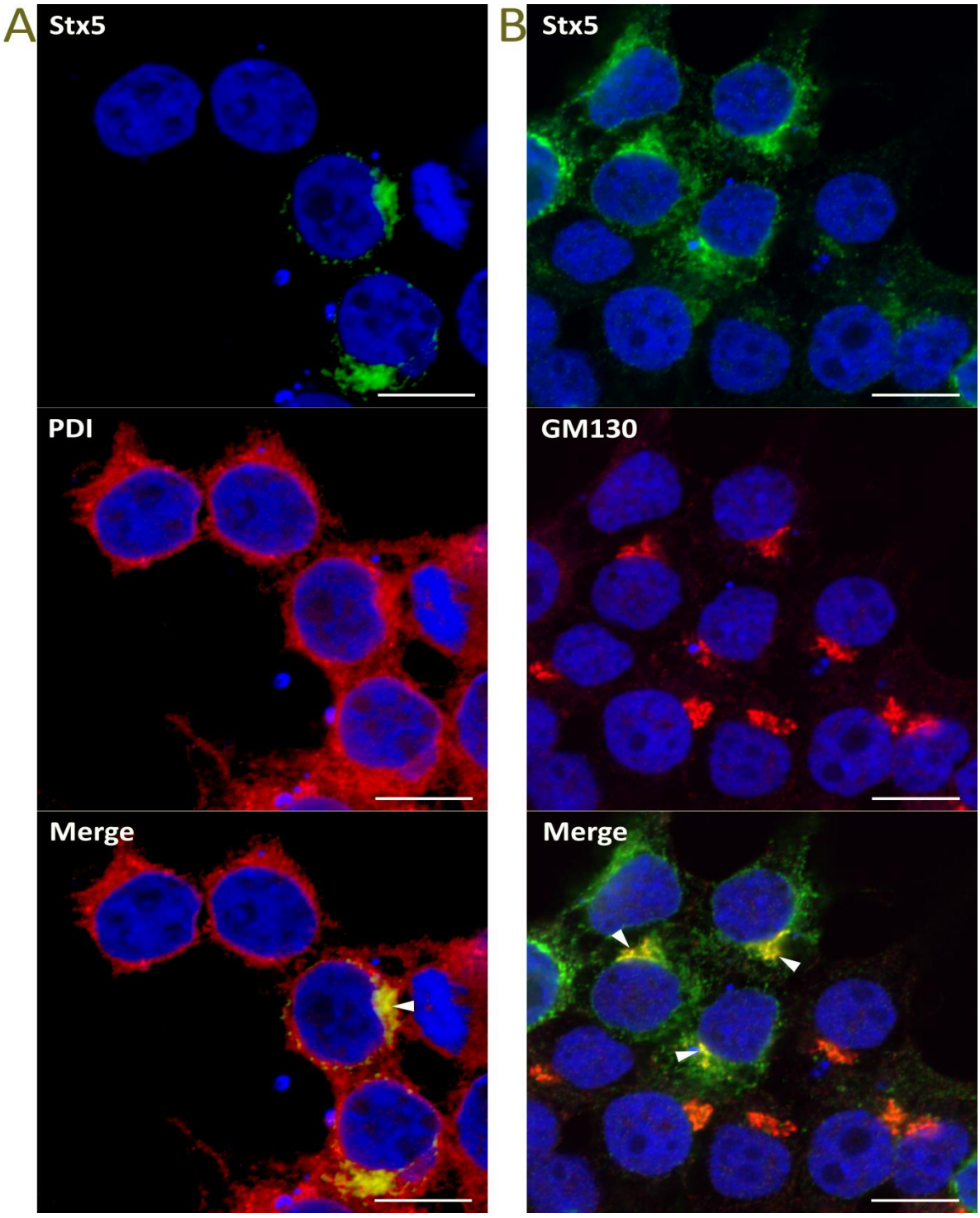

Figure 8 Co-immunostainings of Stx5 with ER marker PDI and *cis*-Golgi marker GM130. HEK293T cells were transiently transfected with Stx5 in pCMV6-XL5, fixed in paraformaldehyde and co-immunostained with rabbit anti-Stx5 antibody 2604 and mouse anti-PDI (A) or mouse anti-GM130 (B), followed by incubation with respective AlexaFluor488 and AlexaFluor546 conjugated secondary antibodies. The green fluorescence represents Stx5 (A and B), red fluorescence PDI (A) or GM130 (B). Nuclei were counterstained using DRAQ5 (*blue*). Co-stainings revealed localisation of Stx5 in perinuclear vesicles representing *cis*-Golgi compartment (B, *Merge, arrowheads*) and ER ribbon (A, *Merge, arrowheads*). Scale bar = 10 µm.

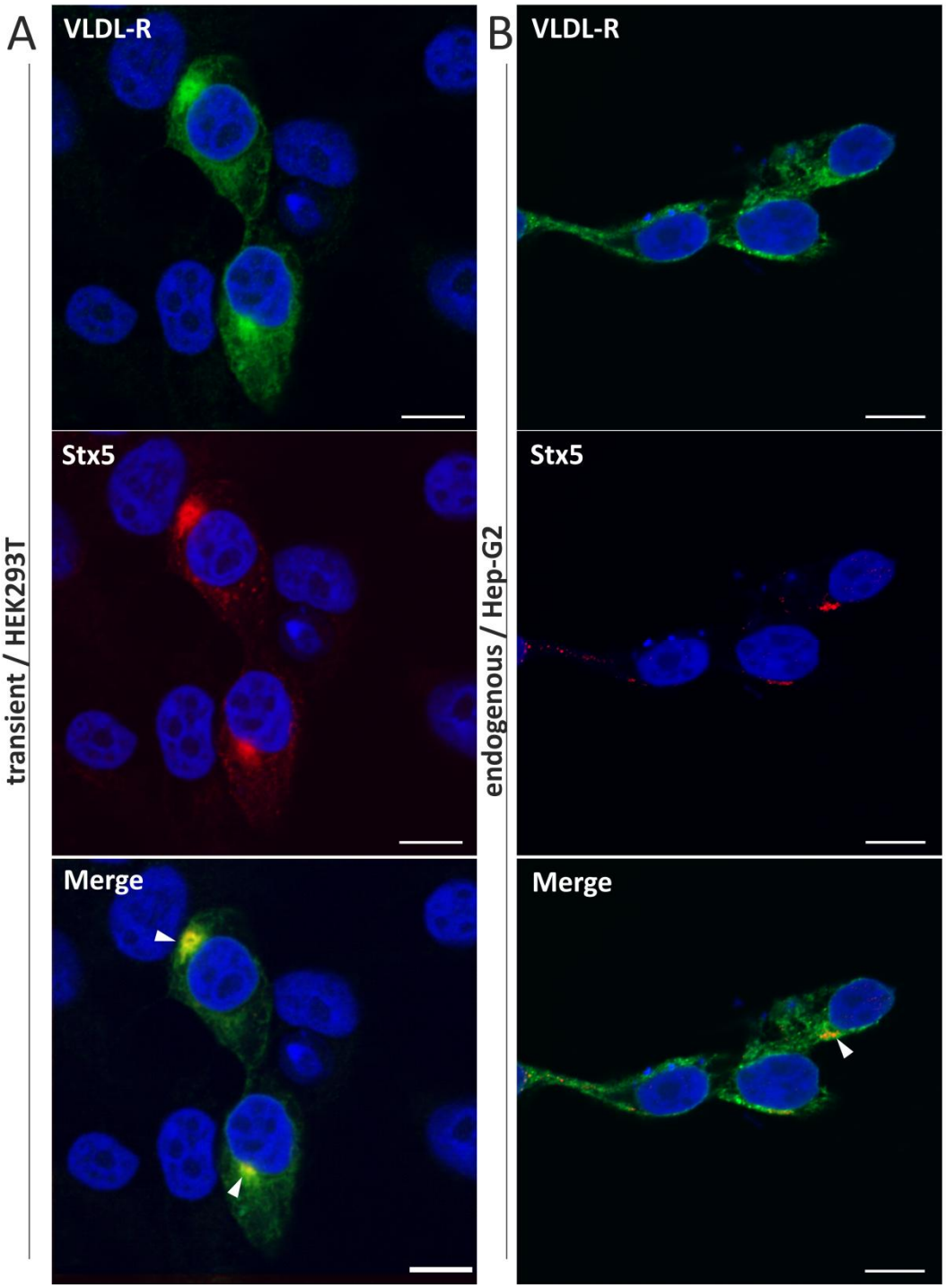

Figure 9 Co-immunostainings of VLDL-R and Stx5. (A) HEK293T cells transiently co-expressing VLDL-R and Stx5 were co-immunostained with 9E10 against myc-tagged VLDL-R and anti-Stx5 antibody 2604, followed by incubation with AlexaFluor488 and AlexaFluor546 conjugated secondary antibody. Nuclei were counterstained with DRAQ5. Co-stainings revealed co-localisation of both proteins in perinuclear regions predominantly representing *cis*-Golgi but also ER vesicles (Merge, arrowheads). (B) To examine co-localisation of endogenous proteins Hep-G2 cells were co-immunostained with mouse anti-VLDL-R antibody 6A6 and anti-Stx5 antibody 2604, followed by incubation with AlexaFluor488 and AlexaFluor546 conjugated secondary antibodies. (A and B) The green fluorescence represents VLDL-R, the red fluorescence Stx5. Proteins were found to co-localise in perinuclear vesicles (*Merge, arrowhead*). Scale bar = 10 µm.

reported for HeLa cells overexpressing the shorter isoform 2 of Sxt5, Stx5S (Suga et al., 2005). In HEK293T cells transiently co-expressing VLDL-R and Stx5 we observed strong co-immunostaining in perinuclear regions representing *cis*-Golgi compartments, but also punctuate vesicular staining possibly resembling ER structures or ER to Golgi intermediate compartments (ERGIC) (Figure 9A, *Merge, arrowheads*). Since endogenous proteins had co-immunoprecipitated in previous Co-IP experiments (Figure 5B), we used liver derived Hep-G2 cells endogenously expressing both VLDL-R and Stx5 to visualise interaction of the two native proteins. We were able to demonstrate co-localisation of endogenous proteins in perinuclear vesicles (Figure 9B, *Merge, arrowhead*).

3.5 Overexpression of Stx5 affects maturation and processing of VLDL-R

Next, we wanted to explore whether Stx5 overexpression might have any detectable effects on VLDL-R. VLDL-R was either co-expressed with Stx5 or expressed alone in HEK293T cells and subsequently analysed by WB (Figure 10A). While solely expressed VLDL-R appeared in two separately migrating bands at approximately 130 kDa (Figure 10A, *middle lane*), representing the mature/fully-glycosylated (*slower migrating band*) and immature/non- or partial-glycosylated (*faster migrating band*) forms of the receptor, co-expression of Stx5 lead to a remarkable reduction in the amount of mature VLDL-R by approximately 75 % (Figure 10A, *left lane* and Figure 10B). Although, VLDL-R maturation seemed to be impaired by richly expressed Stx5, no substantial accumulation of immature protein was observable. Moreover, the reduction in the amount of VLDL-R CTFs of about 80 % in these cells indicated a distinct negative impact of Stx5 on the trafficking and subsequent surface-located processing of the receptor (Figure 10A, *left lane* and Figure 10C). Since several groups claim diverse isoform specific properties of Stx5 and Stx5S (Suga et al., 2009; Miyazaki et al., 2012), we additionally

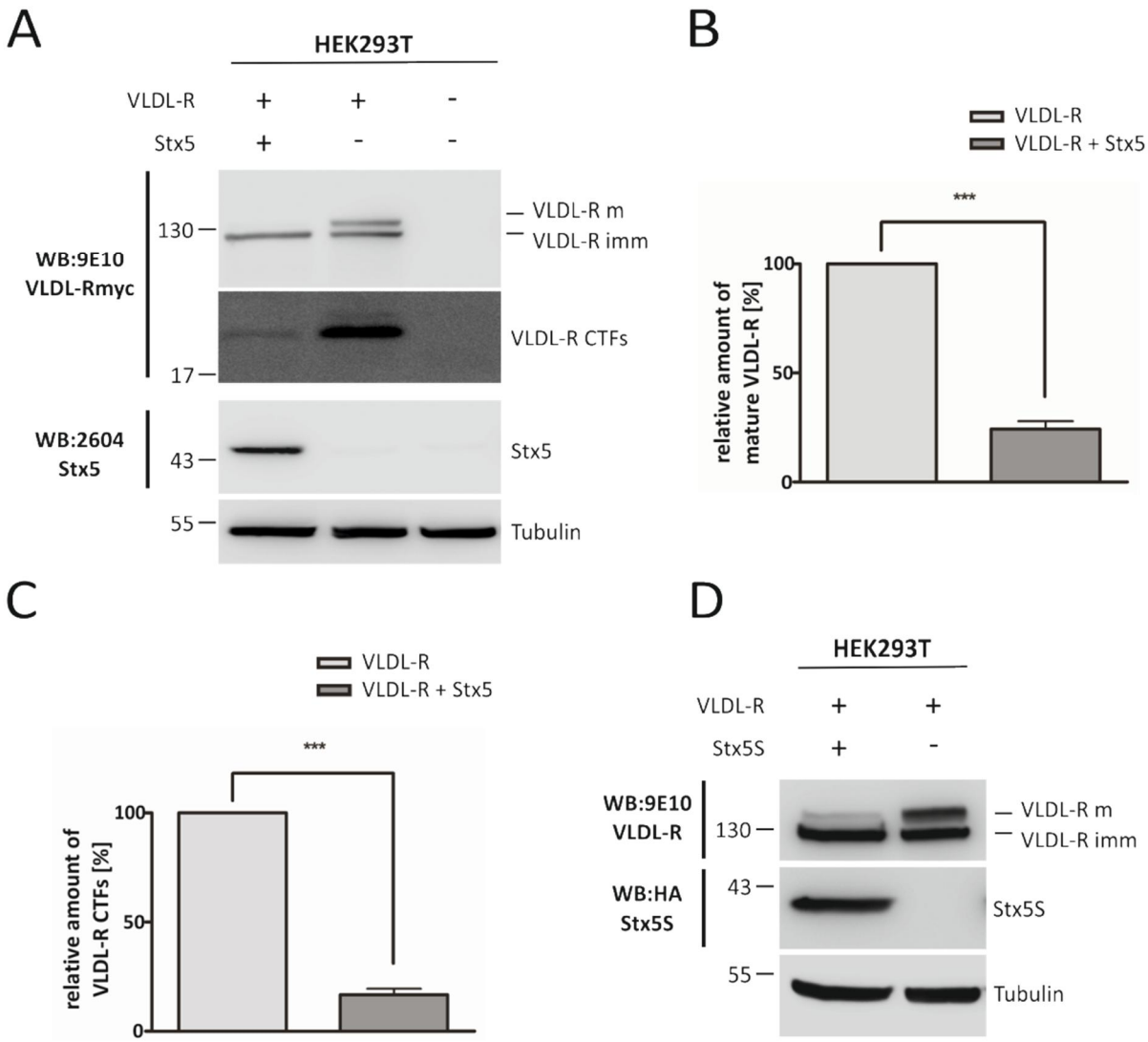

Figure 10 Stx5 overexpression affects maturation and processing of VLDL-R in transiently transfected HEK293T cells. (A) HEK293T cells were transiently co-transfected with myc-tagged VLDL-R in pcDNA3.1A+ and Stx5 in pCMV6-XL5, transfected with VLDL-R or empty vector respectively and analysed by Western blotting. Mature (upper migrating band at ~130 kDa) and immature (lower migrating band at ~130 kDa) forms of VLDL-R and C-terminal fragments (~20 kDa) were detected with 9E10 antibody. Stx5 was detected using anti-Stx5 antibody 2604. Cells overexpressing Stx5 showed dramatically reduced levels of fully glycosylated VLDL-R and C-terminal fragments (CTFs) (A - C). (B and C) Quantification showing relative reduction of mature VLDL-R and CTFs after co-transfection of Stx5, depicted as percentage of vehicle control. Data represents ± SEM as indicated ($n \geq 3$). Statistical significance: ***$p < 0.001$, *t* test. (D) HEK293T cells were either co-transfected with myc-tagged VLDL-R and HA-tagged Stx5S (isoform 2) or VLDL-R and empty vector respectively. Stx5S overexpression impaired VLDL-R maturation in the same manner as Stx5 isoform 1 (A).

examined whether isoform 2, which is the shorter variant of Stx5 (referred to as Stx5S), might affect VLDL-R maturation in a distinct or a similar manner as the longer isoform 1 (Figure 10D). Since the impairment of VLDL-R glycosylation caused by overexpression of Stx5S was evident, we concluded an isoform independent phenomenon. Moreover, we were able to correspondingly observe this effect of Stx5 on the maturation of endogenous VLDL-R in CHOKI cells (Figure 11A). Hence, overexpression of Stx5 significantly reduced the amount of fully-glycosylated VLDL-R by approximately 50 % (Figure 11B). Summing up, the characteristic effect of Stx5 on VLDL-R maturation was similar in cells expressing endogenous or transfected VLDL-R. Still, since the effect was more prominent and therefore easier to read-out when the receptor was overexpressed, further experiments were carried out with transiently transfected myc-tagged VLDL-R.

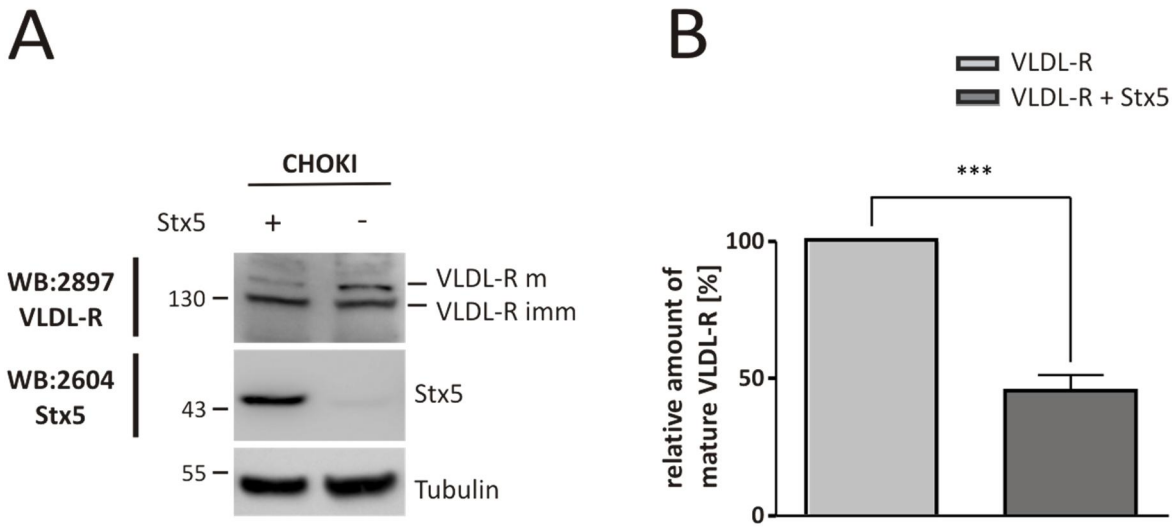

Figure 11 Stx5 overexpression affects maturation of endogenously expressed VLDL-R in CHOKI cells. (A) To examine the effect of Stx5 overexpression on endogenous VLDL-R, CHOKI cells were either transfected with Stx5 or empty vector respectively and analysed by Western blotting. Levels of mature VLDL-R were reduced by Stx5 overexpression compared to vehicle control. Tubulin was used as loading control. (B) Quantification showing relative reduction of mature VLDL-R after co-transfection of Stx5, depicted as percentage of vehicle control. Data represents ± SEM as indicated (n ≥ 3). Statistical significance: ***p < 0.001, *t* test.

3.6 Overexpression of Stx5 effectively prevents VLDL-R maturation

Since Stx5 had such a strong effect on VLDL-R processing we hypothesised, that reduced maturation combined with reduced surface shedding might lead to an altered VLDL-R half-life. We performed pulse-chase analysis using 150 µCi of [^{35}S]-methionine/cysteine and chase periods from 0 h to 72 h (Figure 12). HEK293T cells expressing VLDL-R alone generated considerable amounts of mature VLDL-R after 6 h and the receptor was completely degraded within 72 h (Figure 12A). In contrast, HEK293T cells co-expressing Stx5 displayed a dramatic reduction in the amount of mature VLDL-R by approximately 90 % after 6 h and moreover, did not develop any more maturated protein in the continuance of the experiment (Figure 12B). Interestingly, the pulse-chase study pointed to the retention of VLDL-R in early secretory compartments provoked by high Stx5 expression, but not to an accumulation of immature protein, since the turnover of VLDL-R was not decreased under these circumstances. Immature VLDL-R was nearly completely degraded within 48 h and vanished after 72 h. Moreover, immature VLDL-R seemed to be even faster degraded compared to control cells solely expressing VLDL-R (Figure 12A).

3.7 Immature VLDL-R is degraded by lysosomes and not by ERAD

We considered ER-associated protein degradation (ERAD) of retained VLDL-R as possible explanation for this accelerated turnover of the receptor. Hence, we inhibited proteasomal and also lysosomal degradation prior to a 24-h pulse-chase experiment in HEK293T cells transiently co-expressing VLDL-R and Stx5. Surprisingly, we could not detect any significant increase in the amount of immature VLDL-R after treatment with the proteasome inhibitor MG132, but strong protein accumulation in cells treated with the alkalising agent

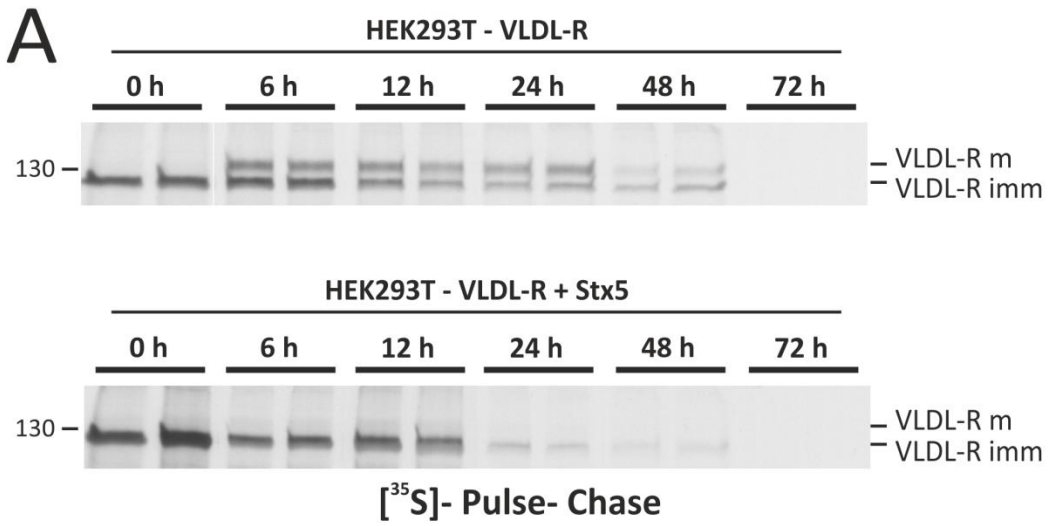

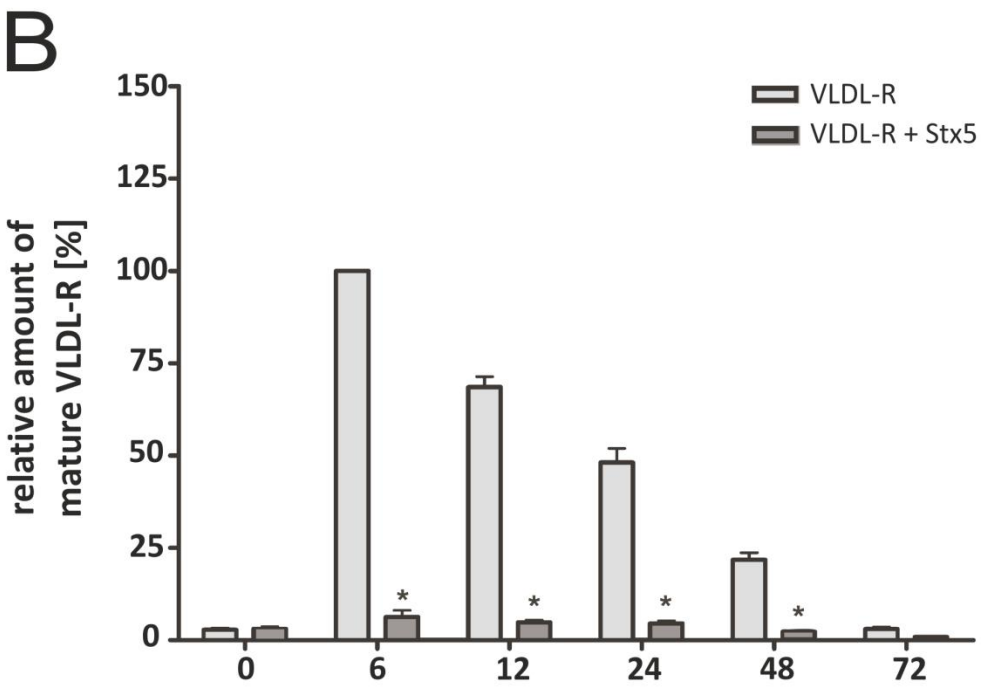

Figure 12 Pulse-chase experiment to analyse the effect of Stx5 on the maturation of VLDL-R through time. (A) HEK293T cells were transiently transfected with myc-tagged VLDL-R in pcDNA3.1A+ alone or co-transfected with Stx5 and pulse-labeled for 30 min with 150 µCi of [^{35}S] methionine/cysteine. Cells were harvested immediately after the pulse (0 h), or chased for the indicated time points with non-radioactive medium. VLDL-R was immunoprecipitated using 9E10 antibody and subjected to SDS-PAGE followed by autoradiography on an X-ray film at -80 °C for a minimum of 12 h. VLDL-R mature and immature forms are indicated. Duplicates represent two independently performed experiments. Note that maturation of VLDL-R in Stx5 transfected cells was almost completely suppressed. (B) Diagram representing the relative changes in the amount of mature VLDL-R in the presence of overexpressed Stx5, quantified as percentage over vehicle control. Mature VLDL-R at 6 h time point was set as 100 %. Data are ($n \geq 3$) ± SEM with a statistical significance of *$p < 0.001$, determined by two-way ANOVA and the Bonferroni post hoc test.

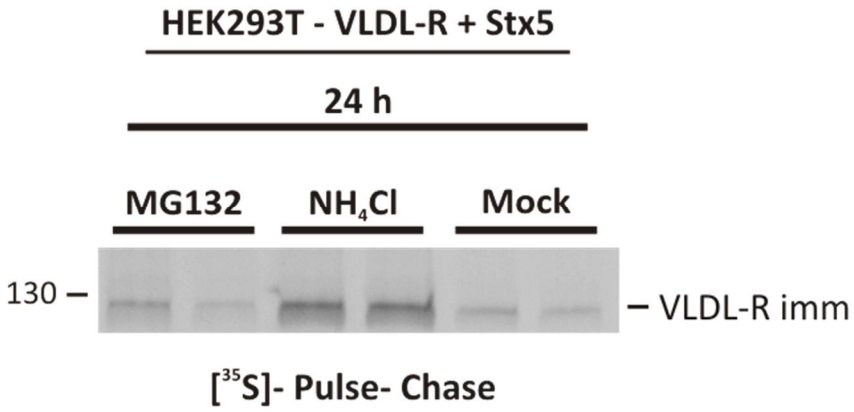

Figure 13 Inhibition of lysosomal and proteasomal degradation of VLDL-R in the presence of Stx5. Prior to [^{35}S] pulse-chase HEK293T cells overexpressing VLDL-R and Stx5 were either treated with 50 µM MG132 for 4 h or 10 mM NH_4Cl for 12 h, respectively. NH_4Cl treated cells showed increased amounts of immature VLDL-R compared to MG132 or non-treated cells at time point 24 h. Duplicates represent two independently performed experiments.

NH_4Cl, which is frequently used as a lysosome inhibitor (Figure 13). These results raised the idea that immature VLDL-R was rather translocated to lysosomal compartments, which usually includes internalisation of VLDL-R from the plasma membrane, than retained within early secretory compartments and subsequently degraded by ERAD.

3.8 Stx5 interaction prevents advanced Golgi maturation of immature VLDL-R representing the ER-/N-glycosylated form of the receptor

To assess the efficiency of the predicted interaction between Stx5 and VLDL-R within early secretory compartments, we characterised the glycosylation patterns of VLDL-R in the presence and absence of abundantly expressed Stx5. Therefore, we used Endoglycosidase H (EndoH) and PNGaseF to remove all N-linked carbohydrate moieties attached to proteins in the ER (Maley, 1989). Western blot analysis of digested lysates revealed that with moderate

expression levels of Stx5, VLDL-R migrated as a set of three bands, representing fully glycosylated protein (Figure 14A and B, *lanes 3 and 4, slower migrating band*), ER glycosylated protein (Figure 14A and B, *lane 4, intermediate migrating band*) and the unglycosylated form of the receptor (Figure 14A and B, *lane 3, faster migrating band*).

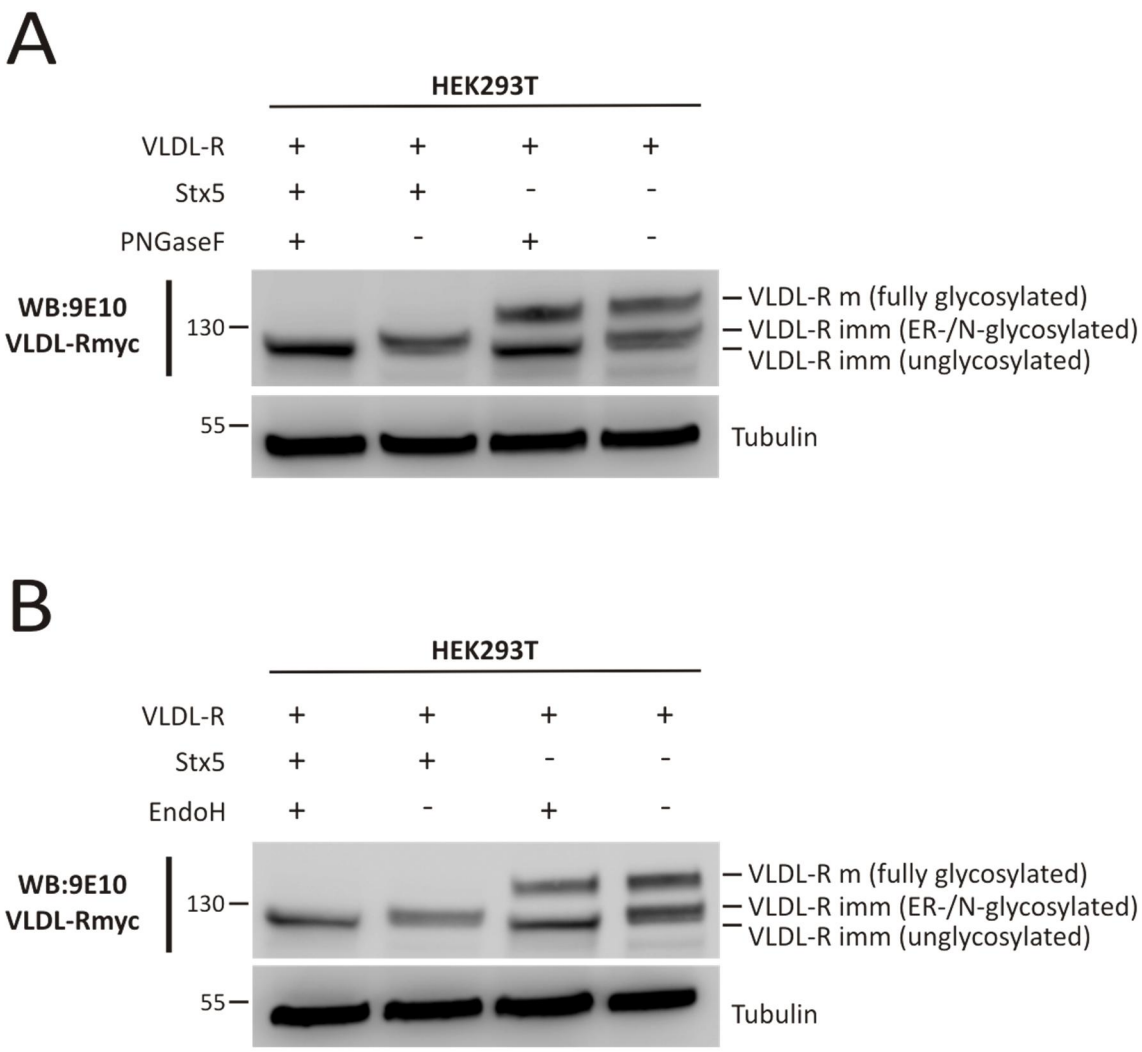

Figure 14 PNGaseF and EndoH digestion of VLDL-R. HEK293T cells were transiently co-transfected with myc-tagged VLDL-R in pcDNA3.1A+ and Stx5 in pCMV6-XL5 or transfected with VLDL-R alone. Prior to analysis by Western blot, 20 µg of each lysate were denatured and digested with PNGaseF (A, lanes 1 and 3) or EndoH (B, lanes 1 and 3). Appropriate samples lacking the enzyme were used as digestion control (A and B, lanes 2 and 4). The different glycosylation stages of VLDL-R are indicated.

Addition of PNGaseF or EndoH removed all N-linked glycans from the ER glycosylated form of VLDL-R leading to a slight accumulation of the unglycosylated receptor. Expectedly, fully glycosylated VLDL-R appeared to be rather resistant against residue removal, due to advanced glycan modifications accomplished within Golgi ribbon. As seen before, overexpression of Stx5 resulted in a complete abolishment of fully-glycosylated VLDL-R (Figure 14A and B, *lanes 1 and 2*). PNGaseF/EndoH digestion lead to a remarkable reduction of the immature form of VLDL-R we detected before (Figure 10A, *lane 1*) to a considerably lower level representing completely unglycosylated protein (Figure 14A and B, *lane 1*). From the observed glycosylation patterns, we concluded that VLDL-R was normally N-glycosylated within the ER, transported to the *cis*-Golgi and then not further Golgi-routed and -modified due to the interaction with exceedingly present Stx5.

3.9 VLDL-R maturation is not impaired by siRNA knock-down of Stx5

We next set out to clarify whether the observed Stx5 effect on VLDL-R maturation was actually attributed to interaction of functional proteins or emerging from disturbed vesicle transport caused by Stx5 overexpression. In a siRNA approach we knocked down the expression of endogenous Stx5 in HEK293T cells, transfected them with VLDL-R, and compared the effect on the maturation of the receptor to cells co-expressing Stx5 by WB (Figure 15A). The quantitative data (Figure 15B) revealed a reduction of mature VLDL-R by ~75 % when Stx5 was overexpressed. However, both concentrations of siRNA (0.2/2 µg/µl) knocked down endogenous Stx5 by approximately 70 % and 90 % compared to scrambled siRNA control but thus had no negative effect on VLDL-R trafficking, since we detected no reduction in the amount of mature VLDL-R. We speculate that Stx5 mediated vesicle transport from ER to Golgi was efficiently compensated by other proteins sharing

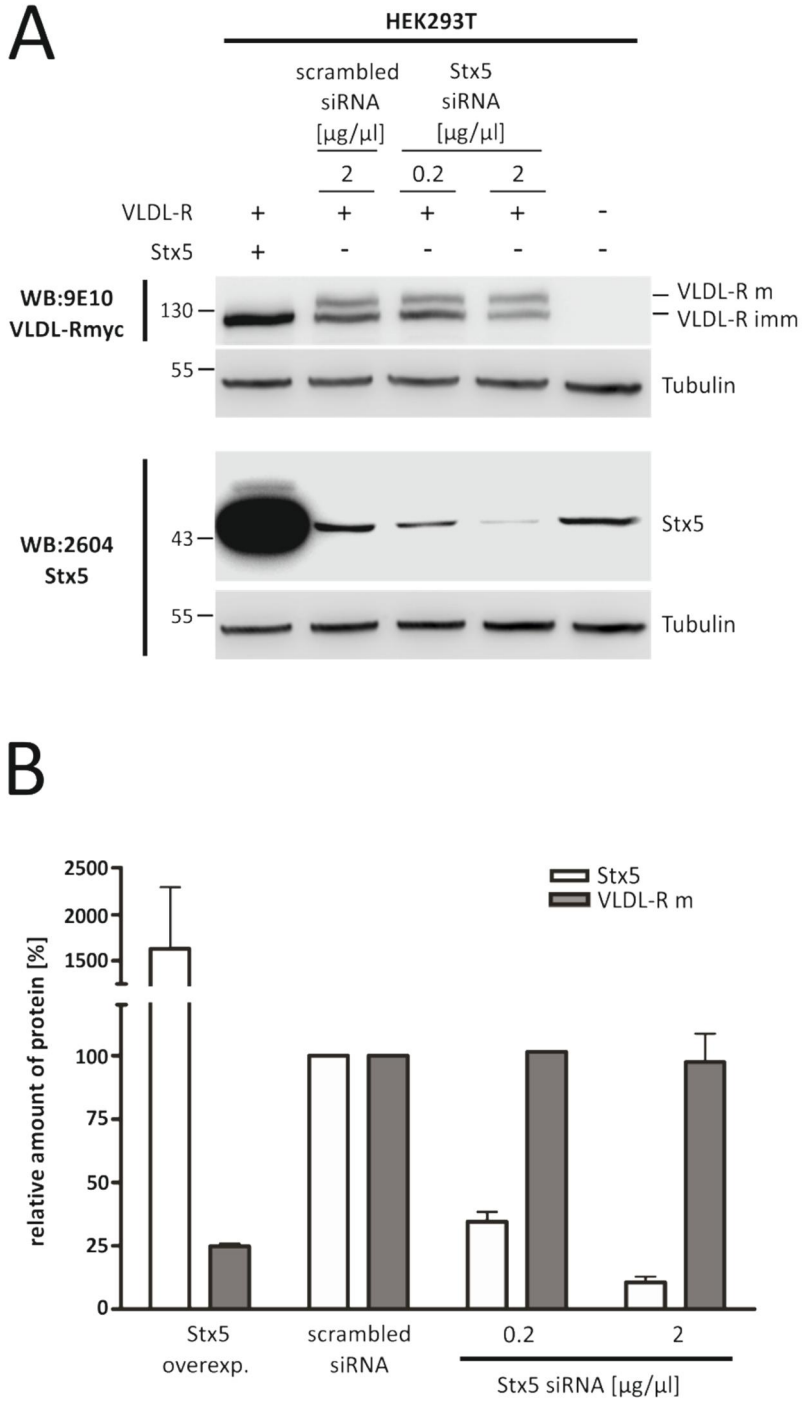

Figure 15 siRNA knock-down does not mimic the overexpression-dependent effect of Stx5 on VLDL-R maturation. (A) HEK293T cells were transiently co-transfected with C-terminally myc-tagged VLDL-R and Stx5 or co-transfected with VLDL-R and Stx5 siRNA in two different concentrations respectively. Co-transfection of VLDL-R and non-targeting scrambled siRNA served as negative control. VLDL-R was detected using 9E10, Stx5 was detected using 2604. Tubulin was used as loading control. Shown is one representative Western blot. (B) Diagram showing relative decrease of mature VLDL-R with varying expression levels of Stx5. Overexpression of Stx5 lead to an immense decrease in the amount of mature VLDL-R, whereas Stx5 knock-down had no effect on the glycosylation pattern of the receptor (n = 2).

functional properties with Stx5. Also, it is possible that the small residual amounts of Stx5 were still sufficient for proper vesicle fusion at the *cis*-Golgi stacks. Taken together, since knock-down of Stx5 did not mimic the overexpression-dependent maturation phenotype of VLDL-R, we concluded that the effect on VLDL-R maturation caused by Stx5 overexpression is reasonably a specific effect on the receptor and cannot be reduced to disturbed COPII vesicle transport resulting from dysfunctional Stx5.

3.10 Stx5 overexpression and knock-down do not affect maturation and processing of LRP1

To further investigate the specificity of the effect of overexpressed Stx5 directly on VLDL-R, we examined the role of Stx5 on the trafficking and processing of another membrane protein, which like VLDL-R is routed anterograde within COPII vesicles from ER to *cis*-Golgi. Therefore, we used LRP1, for which we already had excluded direct binding to Stx5 (Figure 6B). We first studied whether siRNA knock-down of Stx5 might affect trafficking and maturation of LRP1. Therefore, we accomplished Stx5 knock-down and overexpression in CHO 13-5-1 cells stably expressing LRP1 domain IV mini-receptor (mLRP1 IV) and transiently expressing VLDL-R, and calculated the ratios of immature to mature proteins from three independent experiments. A 60 % knock-down of Stx5 was not sufficient to significantly alter the ratios whether of mature to immature VLDL-R (Figure 16A) or LRP1 (Figure 16B). Also in these cells, COPII vesicle transport from ER to Golgi was not disturbed by knock-down of Stx5. In contrast, overexpression of Stx5 resulted in an adequately decreased mature/immature ratio of VLDL-R (Figure 16A) whereas there was no significant effect on LRP1 maturation (Figure 16B). This outcome further strengthened the assumption that Stx5

overexpression may affect VLDL-R directly rather than disturbing entire vesicle transport from ER to Golgi.

To supplementary reject an effect of Stx5 on LRP1, we subsequently examined lysates of HEK293T cells overexpressing Stx5 or mock for processing stages of endogenous LRP1 (Figure 17). In contrast to the observed effect on VLDL-R maturation in these cells (Figure 10), no significant changes in the levels of mature (LRP1 β-chain) or immature LRP1 (LRP1 fl) were detected when Stx5 was overexpressed demonstrating that both trafficking and processing of LRP1 were not influenced by the presence of abundantly expressed Stx5 (Figure 17). Having shown that endogenous LRP1 was not affected, we additionally intended to exclude an artificial effect of Stx5 on overexpressed LRP1. Using 13-5-1 mLRP1 IV cells, we were unable to observe an effect of overexpressed Stx5 either on the mLRP1 IV α-chain

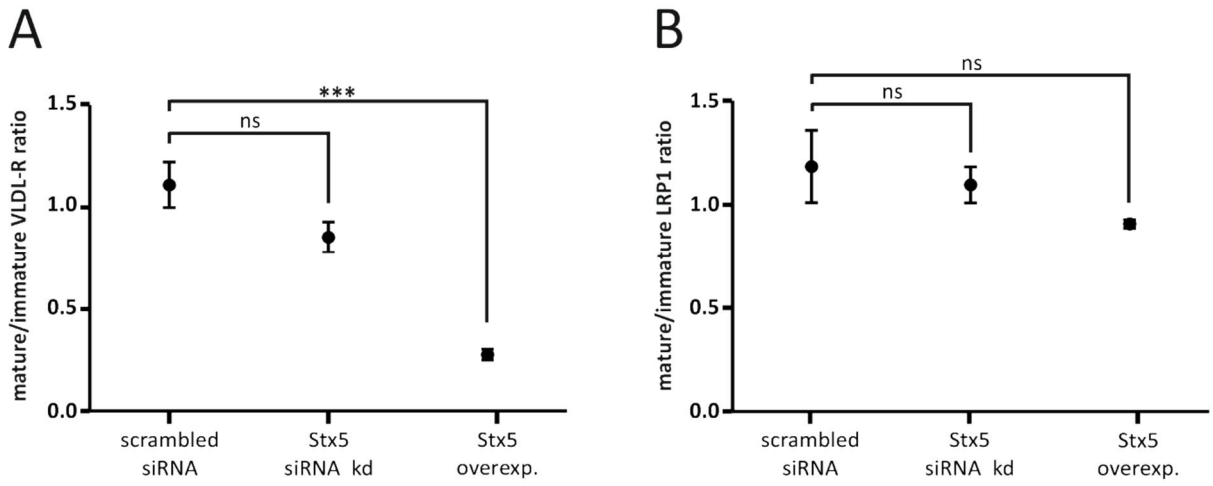

Figure 16 Mature to immature ratios of VLDL-R and LRP1 after Stx5 knock-down or overexpression in 13-5-1 mLRP1 IV cells. (A) Diagram showing the mature/immature ratio of VLDL-R from CHO cells lacking endogenous LRP1 expression (13-5-1) and stably expressing LRP1 domain IV mini-receptor (mLRP1 IV), either transfected with scrambled siRNA, 2 µg/µl Stx5 siRNA or the Stx5 cDNA construct in pCMV6-XL5. Western blot analysis and quantification of the bands representing mature and immature VLDL-R revealed that Stx5 siRNA had no effect whereas overexpression of Stx5 significantly altered the mature/immature ratio of VLDL-R compared to scrambled siRNA control. (B) Examination of the mature/immature ratio of stably expressed mLRP1 IV in 13-5-1 cells revealed statistically significant differences neither for siRNA knock-down nor Stx5 overexpression versus scrambled siRNA control. Data are ($n \geq 3$) ± SEM with a statistical significance of ***$p < 0.001$.

representing the mature form of the receptor or immature protein (mLRP1 IV fl) and moreover, levels of mLRP1 IV CTFs were unaltered (Figure 18A and B). As expected, also in this cell line VLDL-R maturation and processing were dramatically inhibited by co-expression of Stx5 further indicating the specificity of Stx5 interaction with VLDL-R. Since expression levels of VLDL-R and LRP1 were comparably high, we could also reject overexpression artefacts due to exceeding levels of the receptors.

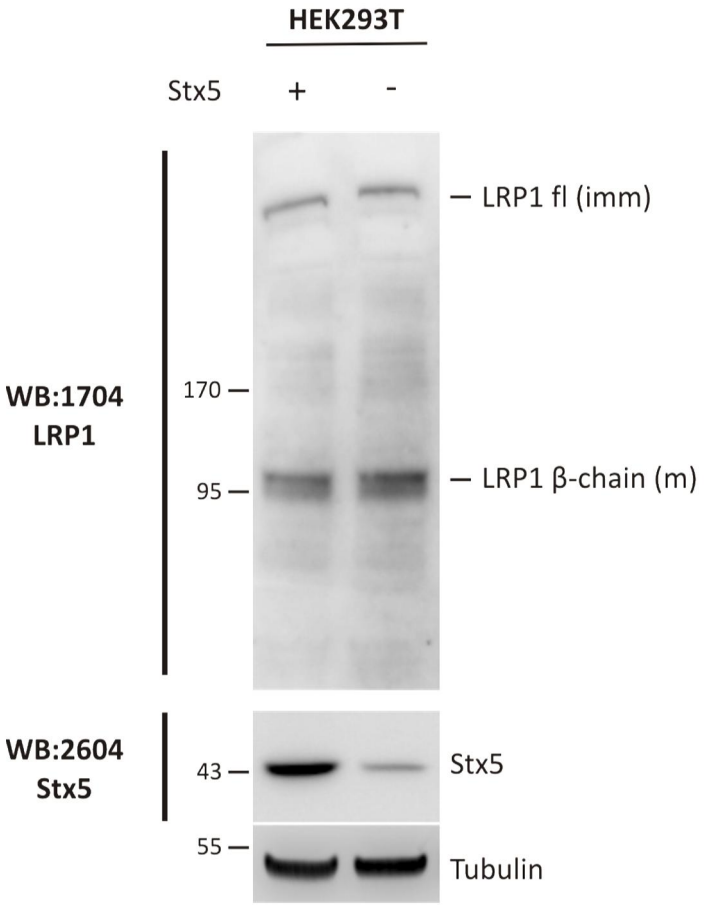

Figure 17 Stx5 overexpression does not impair endogenous LRP1 maturation in HEK293T cells. (A) HEK293T cells were transiently co-transfected with Stx5 or empty vector respectively and analysed by Western blotting. Stx5 was detected with 2604 and endogenous LRP1 with 1704 antibody. Stx5 overexpression had no effect on maturation of endogenously expressed LRP1, taken from unchanged levels of both LRP1 β-chain (mature form of LRP1) and LRP1 fl (immature form of LRP1). Tubulin was used as loading control. Shown is one representative Western blot.

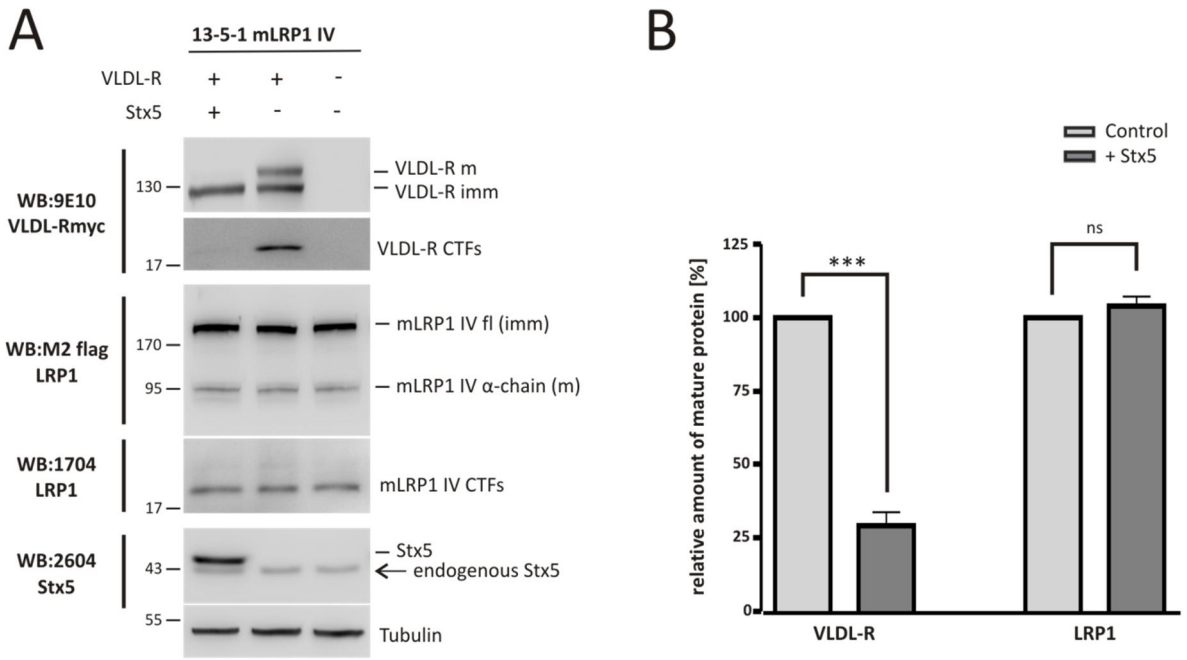

Figure 18 Stx5 overexpression has no effect on LRP1 maturation and processing in 13-5-1 mLRP1 IV. (A) CHO cells lacking endogenous LRP1 expression (13-5-1) and stably expressing LRP1 domain IV mini-receptor (mLRP1 IV) were transiently either co-transfected with VLDL-R and Stx5 or transfected with VLDL-R or empty vector respectively and subsequently analysed by Western blotting. 9E10 antibody was used to detect VLDL-R, Stx5 was detected by using 2604 and flag-tagged mLRP1 IV was visualised using M2 antibody. The arrow indicates endogenous hamster Stx5, migrating marginally faster that human Stx5 likely due to lower molecular weight of hamster Stx5. Note that neither levels of mLRP1 IV α-chain (mature) nor mLRP1 IV CTFs were changed by overexpression of Stx5 whereas the characteristic effect on VLDL-R was clearly visible. Tubulin was used as loading control. Shown is one representative Western blot. (B) Diagram showing the relative amount of mature VLDL-R and LRP1 in 13-5-1 mLRP1 IV overexpressing Stx5 (+ Stx5) compared to non-transfected cells (control). Mature VLDL-R and LRP1 in control cells was set as 100 %. While mature VLDL-R was dramatically reduced by Stx5 expression, levels of fully glycosylated LRP1 remained unaltered compared to control. Data are ($n \geq 3$) ± SEM with a statistical significance of ***$p < 0.001$, determined by two-way ANOVA and the Bonferroni post hoc test.

3.11 Stx5 translocates immature VLDL-R to the cell surface independently from the common secretory pathway

Since inhibition of lysosomal degradation resulted in increased amounts of immature VLDL-R when Stx5 was overexpressed (Figure 13), we addressed the question whether the presence

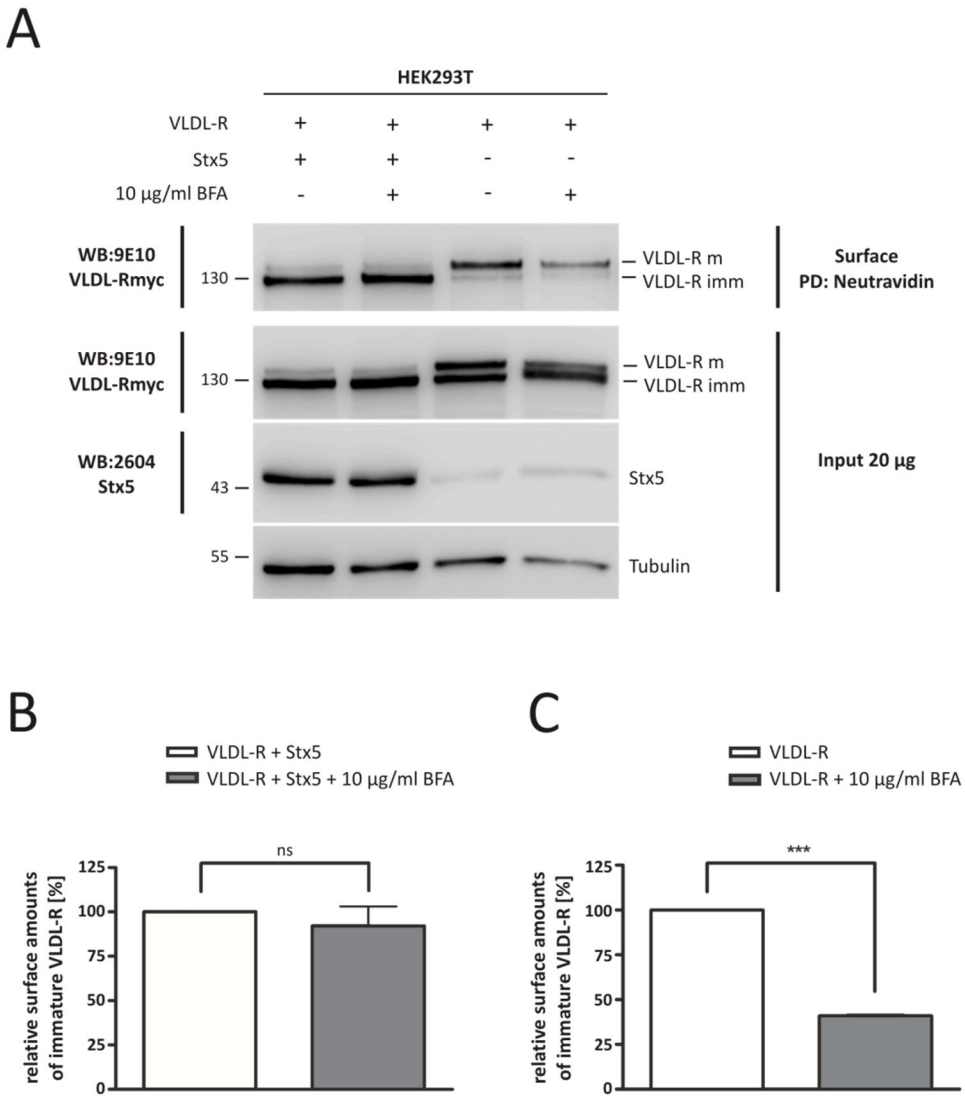

Figure 19 Cell surface expression of immature VLDL-R caused by overexpression of Stx5 is insensitive to BFA treatment. (A) HEK293T cells were transiently co-transfected with myc-tagged VLDL-R and Stx5 or transfected with VLDL-R respectively. 20 h after transfection cells were treated with 10 µg/ml brefeldin A (BFA) for 4 h and left on 37 °C along with untreated control cells. 24 h post transfection cells were labeled using sulfo NHS-LC-LC-biotin and biotinylated samples were precipitated with NeutrAvidin agarose beads. VLDL-R was detected with 9E10 antibody and co-expression of Stx5 was verified by using anti-Stx5 antibody 2604. Tubulin served as a loading control. For detection of surface proteins, NeutrAvidin beads were treated with reducing loading buffer and heated on 95 °C. Samples were separated on 10 % tris-glycine gels. Note that overexpression of Stx5 resulted in a remarkable amount of immature VLDL-R appearing at the cell surface. Shown is one representative Western blot. (B) Quantification showing relative amount of immature VLDL-R at the cell surface when co-transfected with Stx5. Note that treatment with BFA had no influence on the amount of protein reaching the cell surface. (C) Diagram representing the relative amount of mature VLDL-R at the cell surface when transfected alone. BFA treatment reduced the surface amount of fully glycosylated receptor to 40 % compared to untreated control cells. Data represents ± SEM as indicated ($n \geq 3$). Statistical significance: ***$p < 0.001$, *t* test.

of Stx5 might provoke modified surface expression of the receptor. To visualise the surface expression of VLDL-R we performed a biotinylation approach and subsequent Western blot analysis (Figure 19A). We detected immature but almost no maturated form of VLDL-R

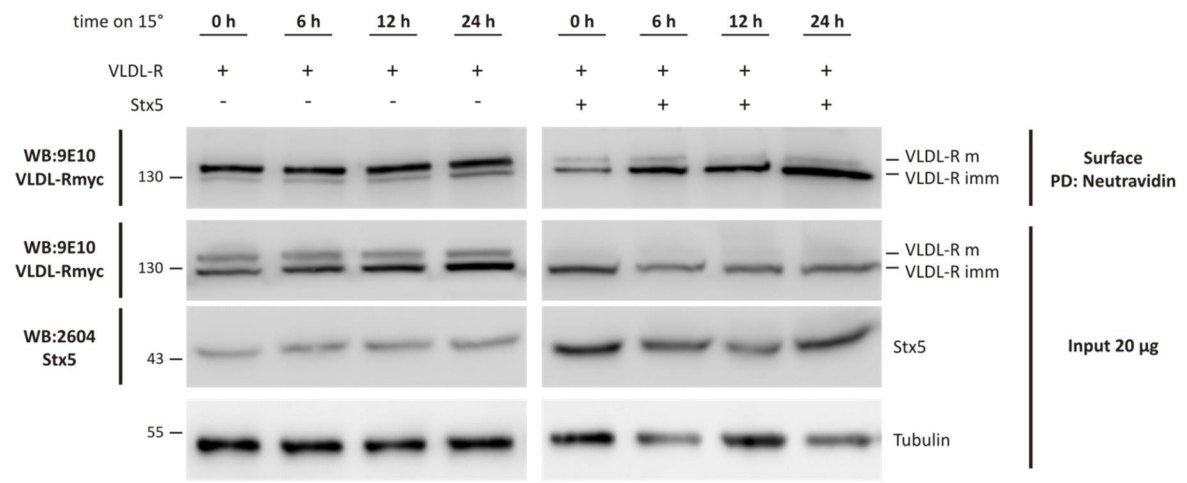

Figure 20 Cell surface expression of immature VLDL-R observable after overexpression of Stx5 is insensitive to incubation at low temperature. HEK293T cells transiently transfected for 24 h with myc-tagged VLDL-R in pCDNA3.1A+ and either Stx5 in pCMV6-XL5 or empty vector, were cultured for indicated time points (h) at 15°C. Cells were labeled with sulfo NHS-LC-LC-biotin and precipitated with NeutrAvidin agarose beads. Biotinylated samples and cell lysates were separated on 10% tris-glycine gels and analysed on Western blot. Myc-tagged VLDL-R was detected with 9E10 antibody and Stx5 was stained with 2604. Tubulin served as a loading control. In cells suffered from low temperature Stx5 overexpression resulted in an increase of immature VLDL-R surface expression through time, along with simultaneous consistent amounts of immature VLDL-R in the lysates. Whereas cell surface amounts of mature VLDL-R in control cells remained unaltered, an increase in immature VLDL-R was observable, both in lysates and at the cell surface.

reaching the cell surface when Stx5 was abundantly co-expressed (Figure 19A, *lane 1*). Using brefeldin A (BFA) we were able to block transport of mature VLDL-R to the cell surface by approximately 60 % in control cells expressing VLDL-R alone (Figure 19A, *lanes 3 and 4*, Figure 19C). In contrast, treatment of VLDL-R and Stx5 co-expressing cells with BFA did not result in a significant reduction of surface expressed immature VLDL-R (Figure 19A, *lane 2*, Figure 19B). We therefore concluded that the interaction of Stx5 with VLDL-R within ER to

cis-Golgi compartments might lead to an export of VLDL-R from the common secretory pathway and direct translocation of the ER-/N-glycosylated receptor to the cell surface.

To further strengthen this assumption, we analysed surface levels of VLDL-R in cells cultured at 15°C for different time periods. Since incubation of cells at 15°C efficiently blocks transport through secretory compartments, we detected no remarkable increase of mature VLDL-R in control cells from time point 0 to 24 h (Figure 20, *left block*). Simultaneously, intracellular immature VLDL-R accumulated with time and was also found to gradually increase at the cell surface. The latter was even more prominent in cells overexpressing Stx5, while there was no accumulation in lysates (Figure 20, *right block*). Based on these findings, we conclude that Stx5 can efficiently export immature VLDL-R to the cell surface independently from common vesicle transport along the secretory pathway.

Given that ER-/N-glycosylated VLDL-R missing Golgi glycosylation was translocated to the cell surface, we examined whether VLDL-R would indeed not appear in *trans*-Golgi areas under Stx5 overexpressing conditions. In order to distinguish between different Golgi areas, we used a continuous 5-25 % iodixanol gradient established by Siman and Velji, which provided complete resolution of the lighter *trans*-Golgi network (TGN) from *cis*-Golgi ribbon (Siman and Velji, 2003). Analysis of membrane distribution of VLDL-R in cells with either high or moderate expression levels of Stx5 was carried out after WB using antibodies marking particular secretory organelles and substructures (Figure 21). With endogenously expressed Stx5, VLDL-R was present in all secretory compartments, determined by calnexin representing ER (fractions 5-11), GM130 marking *cis*-Golgi ribbon (fractions 2-6) and TGN46 indicating the *trans*-Golgi network (fractions 1 and 2) (Figure 21A). Moreover, advanced glycosylation of VLDL-R within Golgi compartments could evidently be monitored by appearance of the slower-migrating band at approximately 130 kDa (fraction 6). As

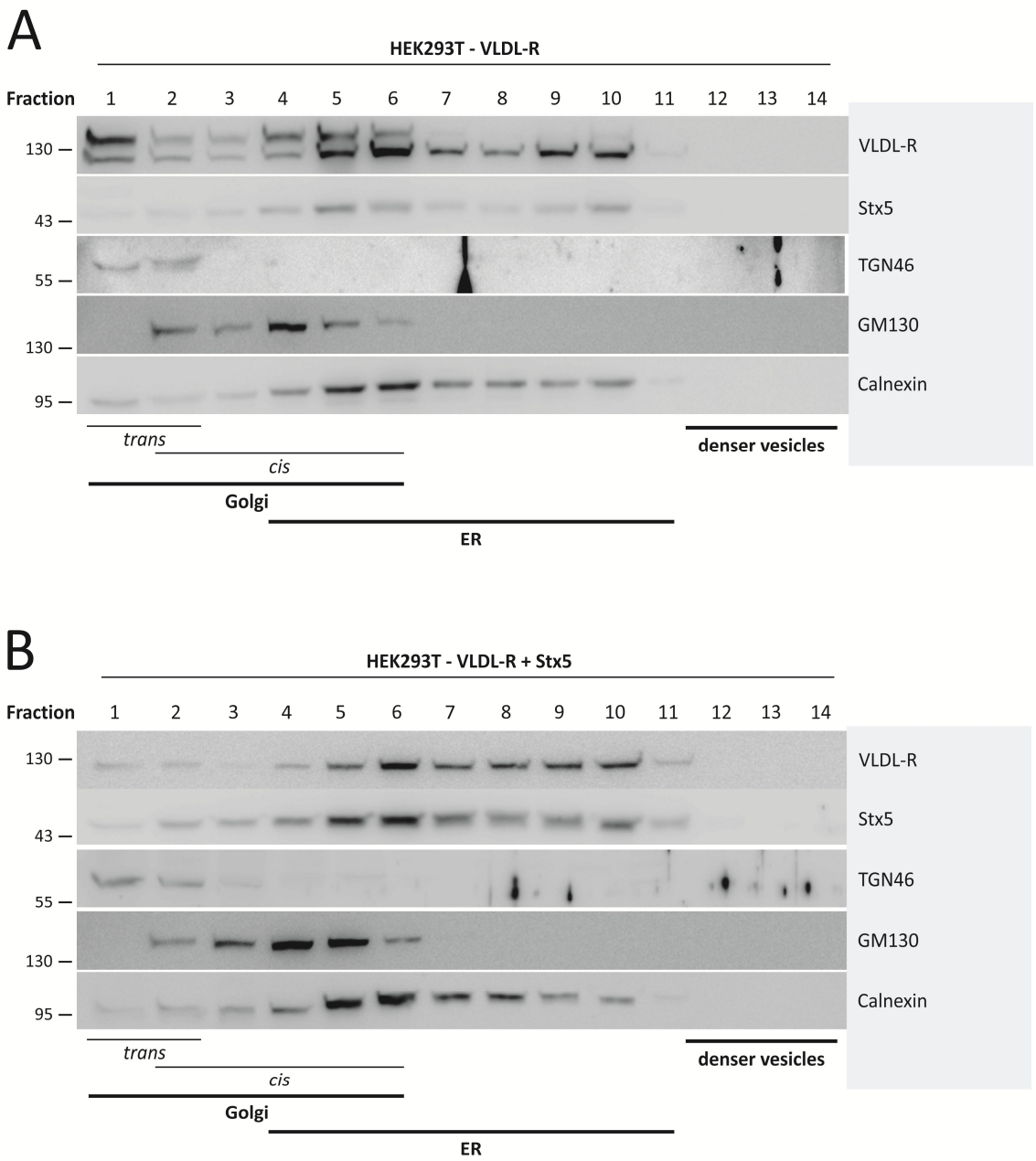

Figure 21 Differential subcellular distribution of VLDL-R in early secretory compartments with abundant or moderate expression levels of Stx5. HEK293T cells were transiently transfected with myc-tagged VLDL-R (A) or co-transfected with VLDL-R and Stx5 (B), respectively. Cell homogenates were layered upon 5-25 % iodixanol gradients and ultra-centrifuged for 3 h. Fourteen 900 µl fractions were collected and 30 µl of each fraction were analysed by Western blotting. Myc-tagged VLDL-R was detected with 9E10 antibody and Stx5 with 2604. TGN46 and GM130 served as *trans*- and *cis*-Golgi indicators and calnexin was used to mark ER ribbon. (A) VLDL-R was found in all fractions representing secretory compartments (fractions 1-11), whereas Stx5 was present in ER to *cis*-Golgi fractions (2-11). The abundant presence of VLDL-R in *trans*-Golgi fraction 1 (A) was diminished when Stx5 was overexpressed (B). Moreover, the slight decrease in the amount of overall VLDL-R from *cis*-Golgi fraction 6 to 3 observed in cells solely overexpressing VLDL-R (A) was comparatively stronger when Stx5 was overexpressed (B), pointing to Stx5-mediated export of VLDL-R from the secretory pathway at the ER exit site, ERGIC vesicles or the initial *cis*-Golgi area.

expected, both endogenous and overexpressed Stx5 was enriched throughout ER to *cis*-Golgi areas (Figure 21A and B). Overexpression of Stx5 significantly altered both, maturation and subcellular distribution of VLDL-R (Figure 21B). The receptor was not further glycosylated through ER to *cis*-Golgi fractions (5-11) and moreover, the amount of VLDL-R was dramatically reduced and barely detectable in TGN fractions (1 and 2) compared to cells solely expressing VLDL-R. Although in general, the amounts of total VLDL-R continuously decreased from *cis*-Golgi fraction 6 to 3 in control cells (Figure 21A), thus was enhanced by Stx5 overexpression (Figure 21B). Consequently, Stx5 seemed to impede VLDL-R trafficking through Golgi compartments, indicating a Stx5-mediated export of VLDL-R from the common secretory pathway at the ER exit site, in ERGIC regions or at the initial *cis*-Golgi stacks.

Fraction	Iodixanol [%]; VLDL-R	Iodixanol [%]; VLDL-R + Stx5
1	8	7.5
2	10.5	10.5
3	12	12
4	13	13
5	15	15
6	17	16.5
7	18	18
8	18	18.5
9	19	19
10	21	21
11	22.5	22.5
12	23.5	23.5
13	23.5	23.5
14	25	25

Table 4 Measured percentage content of iodixanol in the collected subcellular fractions. Refractometric analysis revealed similar concentrations of iodixanol in the collected fractions from both continuous gradients.

Finally, to ensure comparability of the particular fractions collected of both gradients, we measured the percentage content of iodixanol in each fraction (Table 4). Expectedly, concentrations of iodixanol, ranging from 8 % in fraction 1 to 25 % in fraction 14, were virtually identical when comparing respective fractions from the two different gradients.

Taken together, these findings confirmed the assumption that Stx5 might export immature ER-glycosylated VLDL-R from the early secretory pathway directly to the cell surface.

3.12 Confinement of the Stx5 binding site in the cytoplasmic tail of VLDL-R

We finally set out to margin a potential binding site for Stx5 in the cytoplasmic tail of VLDL-R. Since most intracellular adaptor proteins known to interact with VLDL-R require the NPxY (NPVY) motif for proper binding, we assumed that Stx5 might also interact with VLDL-R via this domain. To confirm this hypothesis we constructed a mutated VLDL-R, exchanging the amino acids at position 834 - 837 (Asparagine – Proline – Valine - Tyrosine) against alanines and screened for the characteristic Stx5 effect on the maturation of VLDL-R and the production of VLDL-R CTFs (Figure 22). Overexpression of Stx5 in HEK293T cells transiently transfected with mutated VLDL-R NPVY→AAAA resulted in an immense reduction of maturated VLDL-R, comparable to levels of fully glycosylated wild-type VLDL-R in Stx5 expressing cells. Additionally, the simultaneous reduction in VLDL-R CTFs indicated that Stx5 was still capable of binding VLDL-R properly and influence the receptor's trafficking and subsequent processing. Consequently, we reasoned that the interaction of the two proteins does not occur via the NPVY motif in the cytosolic tail of VLDL-R. For future studies, C-terminally truncated deletion mutants of VLDL-R and further alanine mutants will be designed. Analysing the Stx5 effect on the maturation and cell surface appearance of the

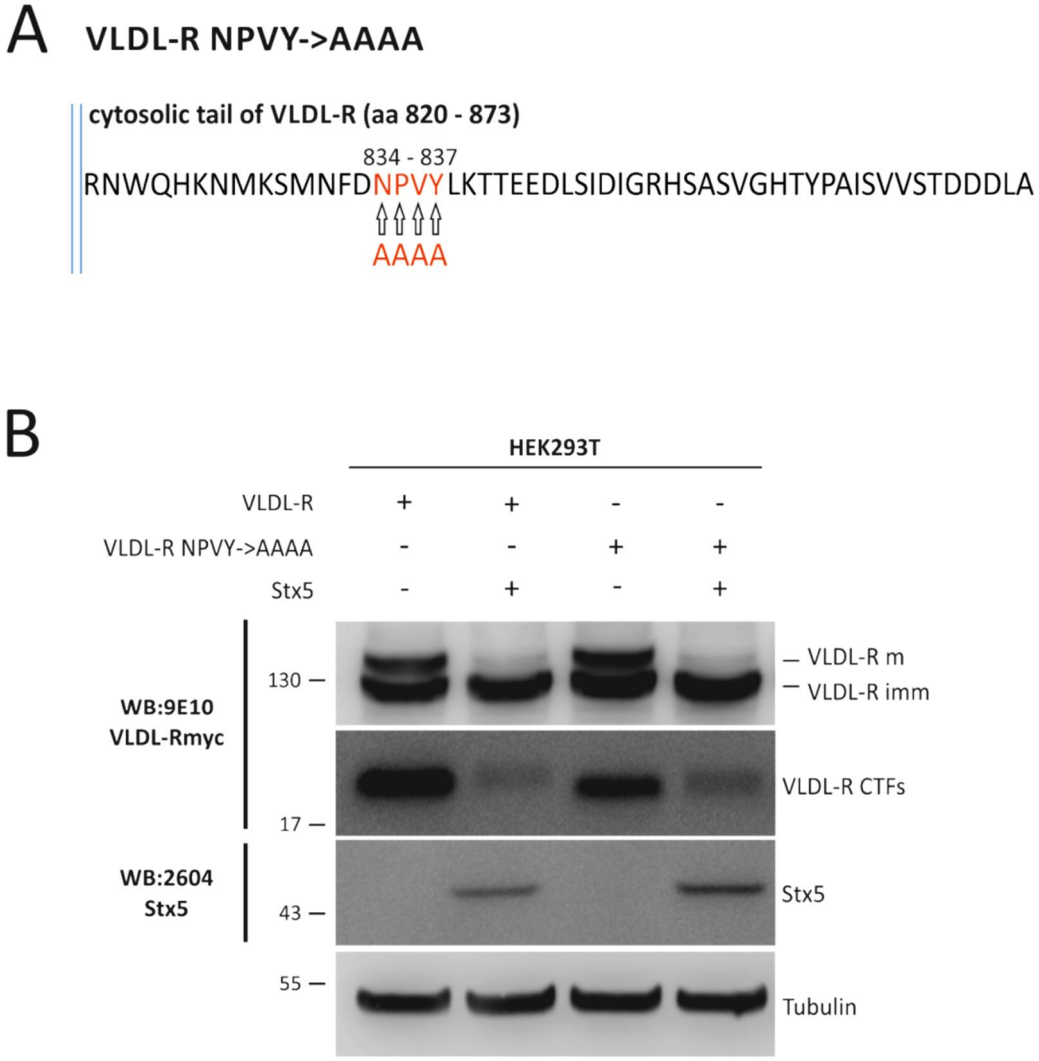

Figure 22 Stx5 interaction does not require a functional NPVY motif in the cytoplasmic tail of VLDL-R. (A) Presented is the amino acid sequence of the cytoplasmic tail of the VLDL-receptor. The membrane is illustrated as a blue double-line. The arrows indicate the positions for the amino acid exchanges (aa 834 - 837). The generated construct was termed VLDL-R NPVY→AAAA. (B) HEK293T cells transiently transfected for 24 h with myc-tagged VLDL-R or VLDL-R NPVY→AAAA in pCDNA3.1A+ and either Stx5 in pCMV6-XL5 or empty vector. Both, full-length protein and CTFs of wild-type and mutated VLDL-R were detected with 9E10 antibody, while Stx5 was stained with 2604. Tubulin served as a loading control. Note that VLDL-R NPVY→AAAA was affected by Stx5 expression in a similar fashion as wild-type VLDL-R.

several constructs should enable us to margin the approximate binding site, or even define the exact motif in the cytosolic part of VLDL-R important for Stx5 interaction.

4 DISCUSSION

4.1 Stx5 is a novel direct interactor of VLDL-R *in vivo* and *in vitro*

The VLDL-receptor is considered as an important participant in brain development and the underlying mechanism is dependent on the interaction of the cell surface receptor with intracellular adaptor proteins. To identify novel interaction partners of VLDL-R, we performed a membrane-based split-ubiquitin yeast two-hybrid screening approach. This technique allowed us to screen for protein-protein interactions between unknown binding partners comprised in a human cDNA library and VLDL-R at the receptors natural site. Based on this *in vivo* method (Johnsson and Varshavsky, 1994) we identified the type IV transmembrane protein Stx5 as a novel interactor binding to the cytoplasmic domain of the VLDL-receptor after exclusion of false-positive interaction by re-transformation procedure (Table 1, Figure 4). To validate this potential interaction *in vitro*, we successfully performed co-immunoprecipitation experiments with both overexpressed and endogenously expressed VLDL-R and Stx5. Since co-immunoprecipitation experiments with membrane bound proteins can lead to false-positive interactions due to co-purification of membrane fractions we additionally performed GST pull-down experiments using the bacterial expressed C-terminal domain of VLDL-R fused to GST as bait. Thereby, we were able to confirm the binding of Stx5 to VLDL-R in these two different experimental approaches (Figure 5 and 6). Most cytosolic adaptor proteins identified so far, binding to the intracellular domains of LDL-receptor family members contain one or more domains known for mediating protein-protein interactions (Gotthardt et al., 2000). For instance, the interaction of Dab1 with VLDL-R's NPxY domain, which is important for the transmission of the reelin signal to migrating neurons in the developing brain is mediated by Dab1's phosphotyrosine-binding (PTB) domain (Howell et

al., 2000). Recently it has been suggested that Fe65, another well-defined binding partner for LDL-receptors might build a complex between VLDL-R and APP by simultaneously interacting with both receptors by its PTB domains (Dumanis et al., 2012). However, those typical NPxY binding motifs are not exclusively essential for intracellular interaction of adaptor proteins with LDL-receptors. For example, ICAP-1 a binding partner for *β*1-integrin lacking such a characteristic domain has been shown to interact with the intracellular domains of LRP1, ApoER2 and Megalin (Gotthardt et al., 2000). Although, the structure of Stx5 includes a t-SNARE coiled-coil homology domain capable of binding other SNARE complex proteins, it remains elusive whether this domain might be involved in VLDL-R binding.

Using a GST fused LRP1 construct comprising the C-terminus of LRP1 as negative control for GST pull-down, we were able to exclude general binding of Stx5 to the cytosolic tails of all LDL-receptors and moreover, since LRP1's cytoplasmic domain contains two NPxY binding motifs, it is evident that most likely a binding site other than the NPxY motif might be important for the Stx5 interaction with VLDL-R. Indeed, alanine (A) substitutions within the NPxY domain of VLDL-R (NPVY→AAAA) caused the same Stx5 dependent maturation phenotype observed when we analysed the effects of Stx5 on wild-type VLDL-R, characterised by tremendously decreased amounts in fully-glycosylated VLDL-R and CTFs (Figure 10, 11 and 22). Accordingly, we conclude that the NPVY motif of the VLDL-receptor is not essential for proper binding and effectiveness of Stx5. Future studies with C-terminally truncated VLDL-R constructs and more alanine mutants might enable us to define the exact motif for Stx5 binding.

To gain further insight into this interaction between Stx5 and VLDL-R, immunocytochemical analyses were performed. These co-localisations revealed the expression of both proteins

within the same intracellular, perinuclear compartments representing the *cis*-Golgi and ER ribbon (Figure 7-9). Consistent with the role of Stx5 in the fusion of anterograde travelling transport vesicles derived from ER compartments, we found that Stx5 vastly localised in *cis*-Golgi cisternae (Dascher et al., 1994). Previously, it had been reported that the overexpression and siRNA knock-down of Stx5 in HeLa cells resulted in the fragmentation of Golgi structures and the accumulation of VSVG-GFP in the ER, suggesting a putative role for Stx5 in maintaining Golgi structure (Suga et al., 2005). Despite using a Stx5 overexpressing system, we could neither detect conspicuous fragmentation of the Golgi in HEK293T cells co-stained with the *cis*-Golgi marker GM130 nor accumulation of VLDL-R within secretory vesicles. Since Suga and colleagues used a shorter variant of Stx5 (isoform 2) differing from our construct (isoform 1), it is thinkable that the observation discrepancies derive from distinct functional properties of the respective isoforms.

Supporting for the assumption that the main localisation site for the association between VLDL-R and Stx5 may be the *cis*-Golgi and/or the exit site of the ER ribbon after N-glycosylation of VLDL-R (Patel et al., 1997), both, PNGaseF and EndoH digestion of VLDL-R revealed that the immature form of the receptor solely appearing when Stx5 was overexpressed represents PNGaseF-/EndoH-sensitive, ER-/N-glycosylated VLDL-R (Figure 14).

4.2 Stx5 affects trafficking of VLDL-R resulting in altered maturation and processing of the receptor

As mentioned in the section above discussing binding site analysis, co-expression of Stx5 with transfected and endogenous VLDL-R resulted in dramatically decreased amounts of fully-glycosylated VLDL-R and VLDL-R CTFs (Figure 10 and 11). Moreover, the effect was isoform independent, since Stx5S impaired maturation of VLDL-R similarly to Stx5 (Figure

10D). Since siRNA knock-down of endogenous Stx5 did not mimic this overexpression-based impairment of VLDL-R maturation (Figure 15), we conclude that the observed maturation phenotype of VLDL-R does not result from functional loss of the SNARE protein and impaired vesicle fusion caused by Stx5 overexpression but rather from specific interaction of VLDL-R with Stx5 and thus is featured and therefore becomes observable by Stx5 overexpression. Moreover, Stx5 siRNA knock-down in 13-5-1 cells overexpressing a mini-receptor of LRP1 (mLRP1 IV), a cell surface receptor transported anterograde from ER to *cis*-Golgi within COPII vesicles like VLDL-R, neither resulted in altered ratios of mature to immature VLDL-R nor mLRP1 IV (Figure 16). The fact that overexpression of Stx5 in these cells highly affected ratios of mature to immature VLDL-R but not mature/immature ratios of LRP1, further strengthens the assumption of a direct effect of Stx5 on VLDL-R, which is independent from Stx5's regular function in COPII vesicle fusion. The finding that knock-down of Stx5 has no effect on the trafficking of vesicles from ER to Golgi is an unexpected one, nevertheless it is conceivable, that the downregulation of Stx5 might be effectively compensated by other undefined proteins sharing similar functional properties with Stx5, or also by the remaining small amounts of Stx5 itself. Since the variant of Stx5 we used in our study (isoform 1) and the shorter form Stx5S, which was not detectable with our 2604 antibody are co-generated from one corporate mRNA (Hui et al., 1997), we assume that we had unselectively knocked-down both isoforms in our siRNA approach and consequently, exclude an isoform dependent compensation mechanism. Anyway, these findings designate that Stx5 may not be indispensable for the anterograde traffic of ERGIC vesicles.

The aspartyl protease γ-secretase is a multi-protease complex assembling of four different proteins: presenilin (PS), nicastrin, APH-1 (anterior pharynx-defective 1) and PEN-2 (presenilin enhancer 2) (Kaether et al., 2006). The γ-secretase complex cleaves substrates

like APP (Haass and De Strooper, 1999), LRP1 or ApoER2 (May et al., 2003). Like ApoER2 and LRP1, VLDL-R prior to γ-secretase processing undergoes cleavage by metalloproteases at the cell surface resulting in the release of soluble forms of the receptor and C-terminal fragments (CTFs) (Hoe and Rebeck, 2005), that can be further internalised and then provide substrate for the γ-secretase complex in the endosomal/lysosomal compartments. Stx5 has been reported to be capable of binding presenilin 1 (PS1) and thereby modulates γ-secretase activity in early secretory compartments (Suga et al., 2004). Since VLDL-R CTFs are further processed by γ-secretase complex (May et al., 2003), the reduction in CTFs in HEK293T cells overexpressing Stx5 (Figure 10) might be based on an activation of the multi-protease complex. However, it is more likely that the decreased CTF levels rather result from reduced amounts of fully-glycosylated VLDL-R serving as substrate for previous ectodomain shedding by metalloproteases at the plasma membrane.

So far, the reduction in the amount of fully glycosylated VLDL-R suggested that the interaction between Stx5 and VLDL-R resulted in inhibited transport of the receptor to the cell surface and subsequent retention of immature protein within ER to *cis*-Golgi cisternae. This phenomenon has previously been observed when PS1 and PS2 holoproteins accumulated in cells transiently transfected with Stx5S (Suga et al., 2004). However, our pulse-chase experiments revealed that Stx5 mediated retention of VLDL-R did not lead to an accumulation of the immature receptor (Figure 12). Moreover, in the presence of abundantly expressed Stx5, immature VLDL-R seemed to be even faster degraded, rather by translocation to lysosomal compartments than ERAD since inhibition of lysosomal degradation resulted in accumulated immature VLDL-R whereas inhibited proteasomal degradation was non-effective (Figure 13). Consistent with our finding that immature VLDL-R was reaching the cell surface insensitive to BFA treatment (Figure 19) and incubation at low

temperature (Figure 20), we suppose that the interaction with Stx5 taking place somewhere between the exit site of the ER and the initial *cis*-Golgi compartments results partly in translocation of the ER-/N-glycosylated receptor to the plasma membrane independent from the common SNARE complex machinery and regular Golgi-routing. In subcellular fractionation experiments, we could support our hypothesis by demonstrating that under Stx5-overexpression conditions VLDL-R barely passed the *cis*- and *trans*-Golgi network (Figure 21).

Our hypothesis is consistent with the above highlighted non-effectiveness of Stx5 overexpression and knock-down on the maturation of LRP1. Mature LRP1 is composed of a 515 kDa and a 85 kDa chain, non-covalently attached and generated by proteolytic cleavage from a 600 kDa precursor protein (Willnow et al., 1996). Responsible for the processing step is furin, a subtilisin-type protease highly active in *trans*-Golgi compartments. We exclude a negative effect of Stx5 overexpression on general vesicle trafficking from ER to Golgi and further Golgi-routing through *medial*- and *trans*-Golgi networks, due to the fact that LRP1, which is also transported in COPII vesicles through ERGIC areas (Appenzeller-Herzog and Hauri, 2006) and moreover, did not interact with Stx5 in neither of our *in vitro* binding studies was normally glycosylated and processed (Figure 17 and 18).

These findings accessory indicate a SNARE-independent, direct effect of Stx5 on VLDL-R circumventing the regular secretory pathway. In an earlier study, it has been postulated that X11, a cytosolic adaptor protein which associates with the cytoplasmic domain of APP in the secretory pathway, is capable of suppressing maturation of APP by preventing entrance of immature APP into the late secretory pathway (Saito et al., 2011). Moreover, the authors observed translocation of the accumulated immature APP from early secretory compartments to the plasma membrane, suggesting a function for X11 in the regulation of

intracellular transport and metabolism of APP by bypassing the Golgi. Conclusively, the group hypothesises the existence of a novel alternative pathway which might be important for the regulation of protein processing. Conceivably, we suggest that Stx5 might play a role in modulating VLDL-R's physiology in an analogue fashion by participating in an abrasively described or even completely novel Golgi-bypass pathway.

4.3 Evidence for a Stx5 dependent Golgi bypass and its potential role in the physiology of VLDL-R

Over the years, trafficking of transmembrane proteins and secretion of peptides containing signal sequences through the classical secretory pathway, which implies ER to *trans*-Golgi organelles has been thoroughly investigated and well-established (Rothman, 1994; Lee et al., 2004). The classical route of transmembrane proteins includes N-glycosylation of their ectodomains in the ER, intra-COPII vesicle transport through ER to *cis*-Golgi cisternae (Lee et al., 2004) and further transport along *medial*- and *trans*-Golgi ribbon, where the proteins undergo extended oligosaccharide modification generating complex N- and O-glycans before reaching their destined membrane, such as the plasma membrane. Nevertheless, recent studies reveal more and more examples of cargo proteins trafficking independently from the classical pathway. All proteins circumventing the common Golgi route share resistance to treatment with the secretory pathway inhibitor BFA and moreover, sensitivity for EndoH digestion. This sensitivity for EndoH derives from missing Golgi-based, complex N-/O-glycan modifications usually added to the ER-specific oligosaccharide core (Medzihradszky, 2005). A recent study for instance, outlines the cell surface appearance of glycoproteins lacking Golgi modifications but possessing those attached in the ER (Tveit et al., 2009).

Several Golgi-bypass pathways are suggested (Wiser et al., 1999; Wiser et al., 1999; Manning-Cela et al., 2003; Marti et al., 2003; Hawes, 2005), although the exact secretion mechanisms beyond are poorly understood. One BFA-resistant protein reaching the cell surface, is the receptor-type tyrosine-protein phosphatase C (PTPRC), also termed CD45 (Baldwin and Ostergaard, 2002). Baldwin and Ostergaard observed CD45 appearance at the cell surface of an EndoH-sensitive and an EndoH-resistant form, corresponding to the ER- and the Golgi-glycosylated protein respectively. Regardless of the question whether this ER-glycosylated CD45 might be functional, the researchers detected three times faster surface-delivery of the EndoH-sensitive CD45. The aspect of fast delivery of proteins to the cell surface might be one important reason for such a Golgi-bypass. Since newly synthesised proteins travel to the surface in a range of 5-15 min (Marie et al., 2008), the granting of direct access of receptors to the plasma membrane by circumventing the common secretory pathway might importantly impact cell physiology. Concerning phagocytosis for instance, rapid delivery of membrane components to the forefront of migrating cells like fibroblast might be based on such an alternative pathway (Bretscher, 1996; Jones et al., 2006).

Another aspect for the delivery of differentially glycosylated proteins to the plasma membrane might be the regulation of protein activity. In the case of CD45, assuming the ER-/N-glycosylated protein has functional properties at the plasma membrane the alternative routing around the Golgi might serve as switch for phosphatase activity (Baldwin and Ostergaard, 2002). Despite numerous examples for alternatively trafficking proteins, almost nothing is known about the particular participants actually achieving the corresponding steps in bypass accounting mechanisms. Our data suggest that beside its regular function in

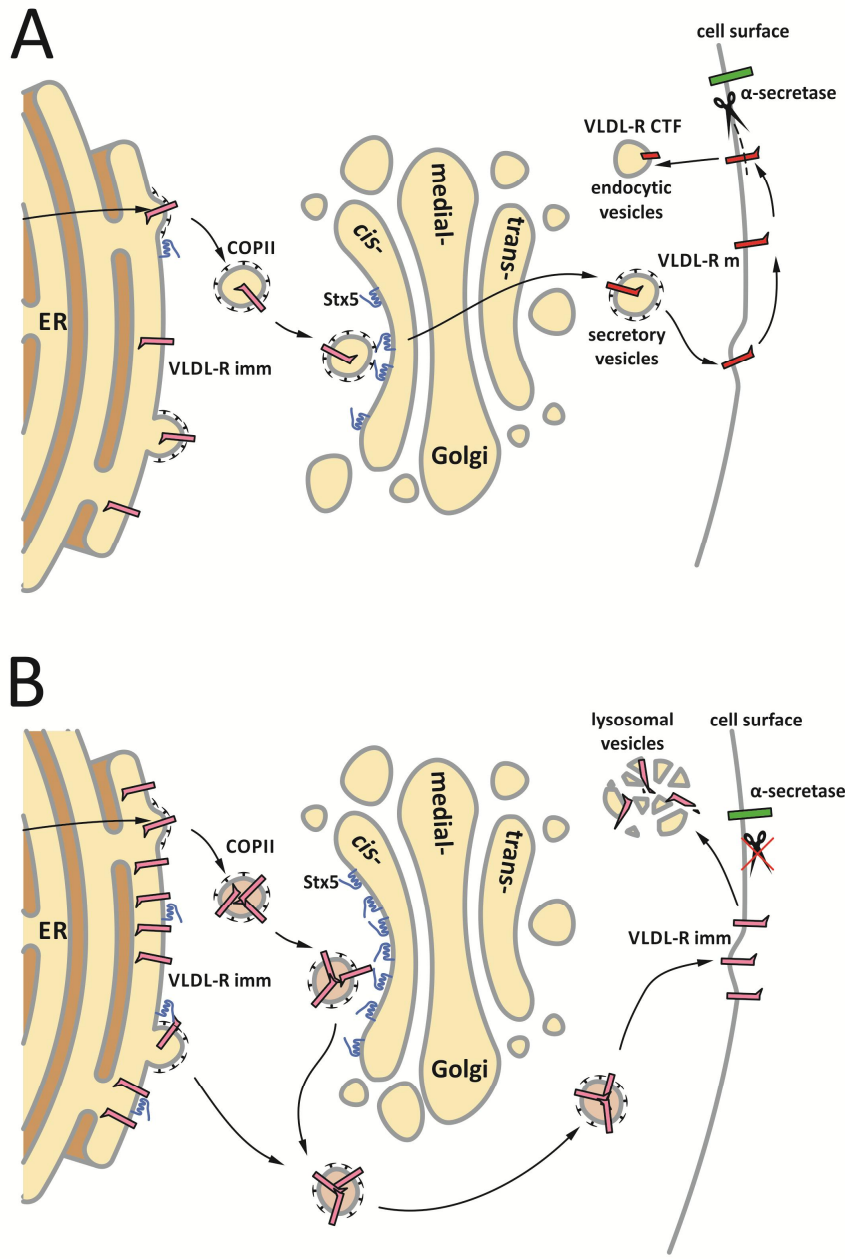

Figure 23 Schematic depiction of VLDL-R trafficking and processing. (A) VLDL-R imm (as depicted in bright red) is transported anterograde within COPII vesicles from ER to *cis*-Golgi compartments, where Stx5 initiates fusion of incoming vesicles with the Golgi membrane by interacting with the SNARE complex machinery. During further *cis*- to *trans*-Golgi transport the receptor is fully glycosylated to VLDL-R m (as depicted in dark red) and subsequently inserted into the plasma membrane at the cell surface, where it can achieve its actual functions and/or serves as substrate for α-secretase cleavage. The processing derived CTFs are retained in the plasma membrane and can be further internalised in endocytic vesicles and then processed by γ-secretase. (B) Upregulation or overexpression of Stx5 (optionally VLDL-R as illustrated here), enhances the probability of both proteins to directly interact with one another. This ER and/or *cis*-Golgi located binding of Stx5 to the cytosolic tail of VLDL-R can lead to subsequent translocation of VLDL-R imm to the cell surface bypassing the common secretory pathway and resulting in reduced surface shedding of the modified receptor due to missing O-glycosylation. This properly non-functional form of the receptor is then abolished by lysosomal degradation.

the conventional secretory pathway, Stx5 may play a putative roll in an alternative pathway by circumventing proteins around the regular Golgi ribbon. Potentially Stx5 concurrently functions in both pathways whereas the equilibrium between these different mechanisms might be regulated by other proteins or the expression levels of Stx5 (Figure 23).

The fact that Stx5 efficiently interacts with VLDL-R and its capability of translocating an ER-maturated form of the receptor to the plasma membrane might have important impacts on the physiology of VLDL-R. May and colleagues demonstrated that differential and tissue-specific glycosylation of LDL-receptors like LRP1 and ApoER2 impacts their sequential processing by secretases and subsequent release of functional relevant cleavage products (May et al., 2003). Consequently, the authors proposed, that alterations in glycosylation might function as a physiological switch influencing the receptors diverse biological functions. Since we could show that Stx5 overexpression alters the glycosylation pattern of VLDL-R, Stx5 might be important in regulating functional VLDL-R expression at the cell surface. In this connection it is of high importance to consider, whether this ER-/N-glycosylated form of VLDL-R could have any considerable function at the plasma membrane. Assuming there is none, Stx5-mediated translocation of this non-functional form of VLDL-R to the cell surface might serve as regulatory switch for VLDL-R activity.

It is as well conceivable, that this novel function of Stx5 might be based on the control and regulation of protein expression levels. ERAD is a mechanism to recognise misfolded and mutated proteins and direct them to proteasomal degradation (Meusser et al., 2005). For analysis of the effect of Stx5 on the maturation of VLDL-R we primarily used a non-mutated and correctly folded cDNA construct of human VLDL-R. Hence, the overexpressed receptor might not be recognised by the proteasome machinery and therefore not designated for ERAD. As observed in this study, the Stx5-mediated translocation of surplus amounts of

VLDL-R to the plasma membrane might counteract overexpression-based ER stress by allowing fast lysosomal degradation of an actually functional but quantitatively not demanded receptor.

The effect of Stx5 on VLDL-R trafficking also implies proximate alteration in the processing of the receptor. The reduction in VLDL-R CTFs, usually deriving from VLDL-R cleavage by metalloproteases indeed points to reduced processing of the full-length construct, possibly because the cell surface appearing immature form missing complex N-glycans and entire O-glycosylation, both accomplished during Golgi passage is not recognised by plasma membrane resident α-secretases (May et al., 2003). Hence, Stx5 might regulate proteolytic receptor cleavage, simply by decreasing the amount of available substrate for the respective secretases. Although our knowledge about the function of lipoprotein receptor CTFs in general remains elusive, it might be worth considering whether decreased VLDL-R CTF levels might have physiological relevance. The release of intracellular domains (ICD) of other cell surface receptors like LRP1 by cleavage of the receptors' CTFs by the γ-secretase complex has been implicated in transcriptional modulation (Kinoshita et al., 2003). This process includes interaction of the ICD with the cytosolic adaptor protein Fe65, recently determined as intracellular linker between VLDL-R and APP (Dumanis et al., 2012). The group proposes a potential translocation of a VLDL-R CTF-Fe65 complex to the nucleus to accordingly function in transcriptional activation, in a similar fashion as LRP1 ICD-Fe65 (Kinoshita et al., 2003).

Concerning decreased α-secretases cleavage of the ER-/N-glycosylated VLDL-R, it is noteworthy that beside the according reduction in VLDL-R CTFs, the extracellular release of the soluble form of the receptor (sVLDL-R), generated by ectodomain shedding of the membrane-bound receptors by metalloproteinases (Rebeck et al., 2006), might as well be affected by Stx5 overexpression. Although, it could be shown that the release of soluble LDL-

receptors can mediate receptor-ligand interactions (Ronacher et al., 2000; Koch et al., 2002; Bajari et al., 2005), the exact functions are poorly understood.

Taken together, the up-regulation of Stx5 expression efficiently alters VLDL-R trafficking and according glycosylation by circumventing the ER-/N-glycosylated receptor around the classical secretory pathway. Therefore, Stx5 might be a key participant in an undetermined Golgi-bypass for VLDL-R to regulate its physiology. According to our findings, it might be interesting to investigate whether Stx5 has an impact on VLDL-R based embryonic development and the organisation of neuronal tissues and structure.

Moreover, for the understanding of the novel bypass it might be of interest to investigate further potential interactors with Stx5.

5 SUMMARY

We identified syntaxin 5 (Stx5), a protein involved in intracellular vesicle trafficking, as a novel interaction partner of the very low density lipoprotein (VLDL)-receptor (VLDL-R), a member of the LDL-receptor family. In addition, we investigated the effect of Stx5 on VLDL-R maturation, trafficking and processing. Here, we demonstrated mutual association of both proteins using several *in vitro* approaches. Furthermore, we detected a special maturation phenotype of VLDL-R resulting from Stx5 overexpression. We found that Stx5 prevented Golgi-maturation of VLDL-R, but did not cause accumulation of the immature protein in ER to Golgi compartments, the main expression sites of Stx5. Rather more, abundantly present Stx5 was capable of translocating ER-/N-glycosylated VLDL-R to the plasma membrane, and thus was insensitive to BFA treatment and incubation at low temperature. Based on our findings, we postulate that Stx5 can directly bind to the C-terminal domain of VLDL-R, thereby influencing the receptor's glycosylation, trafficking and processing characteristics. Resulting from that, we further suggest that Stx5, which is highly expressed in neurons along with VLDL-R, might play a role in modulating the receptor's physiology by participating in a novel/undetermined alternative pathway bypassing the Golgi apparatus.

6 REFERENCES

Appenzeller-Herzog, C and Hauri, HP (2006). "The ER-Golgi intermediate compartment (ERGIC): in search of its identity and function." J Cell Sci 119(Pt 11): 2173-2183.

Arelin, K, Kinoshita, A, Whelan, CM, Irizarry, MC, Rebeck, GW, Strickland, DK and Hyman, BT (2002). "LRP and senile plaques in Alzheimer's disease: colocalization with apolipoprotein E and with activated astrocytes." Brain Res Mol Brain Res 104(1): 38-46.

Bajari, TM, Strasser, V, Nimpf, J and Schneider, WJ (2005). "LDL receptor family: isolation, production, and ligand binding analysis." Methods 36(2): 109-116.

Baldwin, TA and Ostergaard, HL (2002). "The protein-tyrosine phosphatase CD45 reaches the cell surface via golgi-dependent and -independent pathways." J Biol Chem 277(52): 50333-50340.

Beffert, U, Durudas, A, Weeber, EJ, Stolt, PC, Giehl, KM, Sweatt, JD, Hammer, RE and Herz, J (2006). "Functional dissection of Reelin signaling by site-directed disruption of Disabled-1 adaptor binding to apolipoprotein E receptor 2: distinct roles in development and synaptic plasticity." J Neurosci 26(7): 2041-2052.

Bennett, MK, Garcia-Arraras, JE, Elferink, LA, Peterson, K, Fleming, AM, Hazuka, CD and Scheller, RH (1993). "The syntaxin family of vesicular transport receptors." Cell 74(5): 863-873.

Bretscher, MS (1996). "Moving membrane up to the front of migrating cells." Cell 85(4): 465-467.

Burden, JJ, Sun, XM, Garcia, AB and Soutar, AK (2004). "Sorting motifs in the intracellular domain of the low density lipoprotein receptor interact with a novel domain of sorting nexin-17." J Biol Chem 279(16): 16237-16245.

Chao, DS, Hay, JC, Winnick, S, Prekeris, R, Klumperman, J and Scheller, RH (1999). "SNARE membrane trafficking dynamics in vivo." J Cell Biol 144(5): 869-881.

D'Arcangelo, G, Homayouni, R, Keshvara, L, Rice, DS, Sheldon, M and Curran, T (1999). "Reelin is a ligand for lipoprotein receptors." Neuron 24(2): 471-479.

Dascher, C, Matteson, J and Balch, WE (1994). "Syntaxin 5 regulates endoplasmic reticulum to Golgi transport." J Biol Chem 269(47): 29363-29366.

Dumanis, SB, Chamberlain, KA, Jin Sohn, Y, Jin Lee, Y, Guenette, SY, Suzuki, T, Mathews, PM, Pak, D, Rebeck, GW, Suh, YH, Park, HS and Hoe, HS (2012). "FE65 as a link between VLDLR and APP to regulate their trafficking and processing." Mol Neurodegener 7: 9.

Fields, S and Song, O (1989). "A novel genetic system to detect protein-protein interactions." Nature 340(6230): 245-246.

Frykman, PK, Brown, MS, Yamamoto, T, Goldstein, JL and Herz, J (1995). "Normal plasma lipoproteins and fertility in gene-targeted mice homozygous for a disruption in the gene encoding very low density lipoprotein receptor." Proc Natl Acad Sci U S A 92(18): 8453-8457.

Gaisano, HY, Ghai, M, Malkus, PN, Sheu, L, Bouquillon, A, Bennett, MK and Trimble, WS (1996). "Distinct cellular locations of the syntaxin family of proteins in rat pancreatic acinar cells." Mol Biol Cell 7(12): 2019-2027.

Gotthardt, M, Trommsdorff, M, Nevitt, MF, Shelton, J, Richardson, JA, Stockinger, W, Nimpf, J and Herz, J (2000). "Interactions of the low density lipoprotein receptor gene family with cytosolic adaptor and scaffold proteins suggest diverse biological functions in cellular communication and signal transduction." J Biol Chem 275(33): 25616-25624.

Haass, C and De Strooper, B (1999). "The presenilins in Alzheimer's disease--proteolysis holds the key." Science 286(5441): 916-919.

Hawes, C (2005). "Cell biology of the plant Golgi apparatus." New Phytol 165(1): 29-44.

Hay, JC, Klumperman, J, Oorschot, V, Steegmaier, M, Kuo, CS and Scheller, RH (1998). "Localization, dynamics, and protein interactions reveal distinct roles for ER and Golgi SNAREs." J Cell Biol 141(7): 1489-1502.

He, G, Gupta, S, Yi, M, Michaely, P, Hobbs, HH and Cohen, JC (2002). "ARH is a modular adaptor protein that interacts with the LDL receptor, clathrin, and AP-2." J Biol Chem 277(46): 44044-44049.

Hershko, A (2005). "The ubiquitin system for protein degradation and some of its roles in the control of the cell division cycle." Cell Death Differ 12(9): 1191-1197.

Hiesberger, T, Trommsdorff, M, Howell, BW, Goffinet, A, Mumby, MC, Cooper, JA and Herz, J (1999). "Direct binding of Reelin to VLDL receptor and ApoE receptor 2 induces tyrosine phosphorylation of disabled-1 and modulates tau phosphorylation." Neuron 24(2): 481-489.

Hoe, HS, Magill, LA, Guenette, S, Fu, Z, Vicini, S and Rebeck, GW (2006). "FE65 interaction with the ApoE receptor ApoEr2." J Biol Chem 281(34): 24521-24530.

Hoe, HS and Rebeck, GW (2005). "Regulation of ApoE receptor proteolysis by ligand binding." Brain Res Mol Brain Res 137(1-2): 31-39.

Hoe, HS, Tran, TS, Matsuoka, Y, Howell, BW and Rebeck, GW (2006). "DAB1 and Reelin effects on amyloid precursor protein and ApoE receptor 2 trafficking and processing." J Biol Chem 281(46): 35176-35185.

Howell, BW, Herrick, TM, Hildebrand, JD, Zhang, Y and Cooper, JA (2000). "Dab1 tyrosine phosphorylation sites relay positional signals during mouse brain development." Curr Biol 10(15): 877-885.

Hui, N, Nakamura, N, Sonnichsen, B, Shima, DT, Nilsson, T and Warren, G (1997). "An isoform of the Golgi t-SNARE, syntaxin 5, with an endoplasmic reticulum retrieval signal." Mol Biol Cell 8(9): 1777-1787.

Ito, H, Fukuda, Y, Murata, K and Kimura, A (1983). "Transformation of intact yeast cells treated with alkali cations." J Bacteriol 153(1): 163-168.

Jahn, R, Lang, T and Sudhof, TC (2003). "Membrane fusion." Cell 112(4): 519-533.

Johnsson, N and Varshavsky, A (1994). "Split ubiquitin as a sensor of protein interactions in vivo." Proc Natl Acad Sci U S A 91(22): 10340-10344.

Jones, MC, Caswell, PT and Norman, JC (2006). "Endocytic recycling pathways: emerging regulators of cell migration." Curr Opin Cell Biol 18(5): 549-557.

Kaether, C, Haass, C and Steiner, H (2006). "Assembly, trafficking and function of gamma-secretase." Neurodegener Dis 3(4-5): 275-283.

Kasai, K and Akagawa, K (2001). "Roles of the cytoplasmic and transmembrane domains of syntaxins in intracellular localization and trafficking." J Cell Sci 114(Pt 17): 3115-3124.

Kinoshita, A, Shah, T, Tangredi, MM, Strickland, DK and Hyman, BT (2003). "The intracellular domain of the low density lipoprotein receptor-related protein modulates transactivation mediated by amyloid precursor protein and Fe65." J Biol Chem 278(42): 41182-41188.

Kinoshita, A, Whelan, CM, Smith, CJ, Mikhailenko, I, Rebeck, GW, Strickland, DK and Hyman, BT (2001). "Demonstration by fluorescence resonance energy transfer of two sites of interaction between the low-density lipoprotein receptor-related protein and the amyloid precursor protein: role of the intracellular adapter protein Fe65." J Neurosci 21(21): 8354-8361.

Koch, S, Strasser, V, Hauser, C, Fasching, D, Brandes, C, Bajari, TM, Schneider, WJ and Nimpf, J (2002). "A secreted soluble form of ApoE receptor 2 acts as a dominant-negative receptor and inhibits Reelin signaling." EMBO J 21(22): 5996-6004.

Krieger, M and Herz, J (1994). "Structures and functions of multiligand lipoprotein receptors: macrophage scavenger receptors and LDL receptor-related protein (LRP)." Annu Rev Biochem 63: 601-637.

Lee, J, Shin, MK, Ryu, DK, Kim, S and Ryu, WS (2010). "Insertion and deletion mutagenesis by overlap extension PCR." Methods Mol Biol 634: 137-146.

Lee, MC, Miller, EA, Goldberg, J, Orci, L and Schekman, R (2004). "Bi-directional protein transport between the ER and Golgi." Annu Rev Cell Dev Biol 20: 87-123.

Magrane, J, Casaroli-Marano, RP, Reina, M, Gafvels, M and Vilaro, S (1999). "The role of O-linked sugars in determining the very low density lipoprotein receptor stability or release from the cell." FEBS Lett 451(1): 56-62.

Manning-Cela, R, Marquez, C, Franco, E, Talamas-Rohana, P and Meza, I (2003). "BFA-sensitive and insensitive exocytic pathways in Entamoeba histolytica trophozoites: their relationship to pathogenesis." Cell Microbiol 5(12): 921-932.

Marie, M, Sannerud, R, Avsnes Dale, H and Saraste, J (2008). "Take the 'A' train: on fast tracks to the cell surface." Cell Mol Life Sci 65(18): 2859-2874.

Marti, M, Li, Y, Schraner, EM, Wild, P, Kohler, P and Hehl, AB (2003). "The secretory apparatus of an ancient eukaryote: protein sorting to separate export pathways occurs before formation of transient Golgi-like compartments." Mol Biol Cell 14(4): 1433-1447.

May, P, Bock, HH, Nimpf, J and Herz, J (2003). "Differential glycosylation regulates processing of lipoprotein receptors by gamma-secretase." J Biol Chem 278(39): 37386-37392.

Medzihradszky, KF (2005). "Characterization of protein N-glycosylation." Methods Enzymol 405: 116-138.

Meusser, B, Hirsch, C, Jarosch, E and Sommer, T (2005). "ERAD: the long road to destruction." Nat Cell Biol 7(8): 766-772.

Mishra, SK, Watkins, SC and Traub, LM (2002). "The autosomal recessive hypercholesterolemia (ARH) protein interfaces directly with the clathrin-coat machinery." Proc Natl Acad Sci U S A 99(25): 16099-16104.

Miyazaki, K, Wakana, Y, Noda, C, Arasaki, K, Furuno, A and Tagaya, M (2012). "Contribution of the long form of syntaxin 5 to the organization of the endoplasmic reticulum." J Cell Sci 125(Pt 23): 5658-5666.

Patel, DD, Forder, RA, Soutar, AK and Knight, BL (1997). "Synthesis and properties of the very-low-density-lipoprotein receptor and a comparison with the low-density-lipoprotein receptor." Biochem J 324 (Pt 2): 371-377.

Pietrzik, CU, Busse, T, Merriam, DE, Weggen, S and Koo, EH (2002). "The cytoplasmic domain of the LDL receptor-related protein regulates multiple steps in APP processing." EMBO J 21(21): 5691-5700.

Pietrzik, CU, Yoon, IS, Jaeger, S, Busse, T, Weggen, S and Koo, EH (2004). "FE65 constitutes the functional link between the low-density lipoprotein receptor-related protein and the amyloid precursor protein." J Neurosci 24(17): 4259-4265.

Rebeck, GW, LaDu, MJ, Estus, S, Bu, G and Weeber, EJ (2006). "The generation and function of soluble apoE receptors in the CNS." Mol Neurodegener 1: 15.

Ronacher, B, Marlovits, TC, Moser, R and Blaas, D (2000). "Expression and folding of human very-low-density lipoprotein receptor fragments: neutralization capacity toward human rhinovirus HRV2." Virology 278(2): 541-550.

Rothman, JE (1994). "Mechanisms of intracellular protein transport." Nature 372(6501): 55-63.

Russo, T, Faraonio, R, Minopoli, G, De Candia, P, De Renzis, S and Zambrano, N (1998). "Fe65 and the protein network centered around the cytosolic domain of the Alzheimer's beta-amyloid precursor protein." FEBS Lett 434(1-2): 1-7.

Saito, Y, Akiyama, M, Araki, Y, Sumioka, A, Shiono, M, Taru, H, Nakaya, T, Yamamoto, T and Suzuki, T (2011). "Intracellular trafficking of the amyloid beta-protein precursor (APP) regulated by novel function of X11-like." PLoS One 6(7): e22108.

Siman, R and Velji, J (2003). "Localization of presenilin-nicastrin complexes and gamma-secretase activity to the trans-Golgi network." J Neurochem 84(5): 1143-1153.

Stagljar, I, Korostensky, C, Johnsson, N and te Heesen, S (1998). "A genetic system based on split-ubiquitin for the analysis of interactions between membrane proteins in vivo." Proc Natl Acad Sci U S A 95(9): 5187-5192.

Suga, K, Hattori, H, Saito, A and Akagawa, K (2005). "RNA interference-mediated silencing of the syntaxin 5 gene induces Golgi fragmentation but capable of transporting vesicles." FEBS Lett 579(20): 4226-4234.

Suga, K, Saito, A, Tomiyama, T, Mori, H and Akagawa, K (2009). "The Syntaxin 5 isoforms Syx5 and Syx5L have distinct effects on the processing of {beta}-amyloid precursor protein." J Biochem 146(6): 905-915.

Suga, K, Tomiyama, T, Mori, H and Akagawa, K (2004). "Syntaxin 5 interacts with presenilin holoproteins, but not with their N- or C-terminal fragments, and affects beta-amyloid peptide production." Biochem J 381(Pt 3): 619-628.

Teng, FY, Wang, Y and Tang, BL (2001). "The syntaxins." Genome Biol 2(11): REVIEWS3012.

Trommsdorff, M, Borg, JP, Margolis, B and Herz, J (1998). "Interaction of cytosolic adaptor proteins with neuronal apolipoprotein E receptors and the amyloid precursor protein." J Biol Chem 273(50): 33556-33560.

Trommsdorff, M, Gotthardt, M, Hiesberger, T, Shelton, J, Stockinger, W, Nimpf, J, Hammer, RE, Richardson, JA and Herz, J (1999). "Reeler/Disabled-like disruption of neuronal migration in knockout mice lacking the VLDL receptor and ApoE receptor 2." Cell 97(6): 689-701.

Tveit, H, Akslen, LK, Fagereng, GL, Tranulis, MA and Prydz, K (2009). "A secretory Golgi bypass route to the apical surface domain of epithelial MDCK cells." Traffic 10(11): 1685-1695.

Ulery, PG, Beers, J, Mikhailenko, I, Tanzi, RE, Rebeck, GW, Hyman, BT and Strickland, DK (2000). "Modulation of beta-amyloid precursor protein processing by the low density lipoprotein receptor-related protein (LRP). Evidence that LRP contributes to the pathogenesis of Alzheimer's disease." J Biol Chem 275(10): 7410-7415.

van Kerkhof, P, Lee, J, McCormick, L, Tetrault, E, Lu, W, Schoenfish, M, Oorschot, V, Strous, GJ, Klumperman, J and Bu, G (2005). "Sorting nexin 17 facilitates LRP recycling in the early endosome." EMBO J 24(16): 2851-2861.

Wagner, T and Pietrzik, CU (2012). "The role of lipoprotein receptors on the physiological function of APP." Exp Brain Res 217(3-4): 377-387.

Waldron, E, Heilig, C, Schweitzer, A, Nadella, N, Jaeger, S, Martin, AM, Weggen, S, Brix, K and Pietrzik, CU (2008). "LRP1 modulates APP trafficking along early compartments of the secretory pathway." Neurobiol Dis 31(2): 188-197.

Willnow, TE, Moehring, JM, Inocencio, NM, Moehring, TJ and Herz, J (1996). "The low-density-lipoprotein receptor-related protein (LRP) is processed by furin in vivo and in vitro." Biochem J 313 (Pt 1): 71-76.

Willnow, TE, Rohlmann, A, Horton, J, Otani, H, Braun, JR, Hammer, RE and Herz, J (1996). "RAP, a specialized chaperone, prevents ligand-induced ER retention and degradation of LDL receptor-related endocytic receptors." EMBO J 15(11): 2632-2639.

Wiser, MF, Grab, DJ and Lanners, HN (1999). "An alternative secretory pathway in Plasmodium: more questions than answers." Novartis Found Symp 226: 199-211; discussion 211-194.

Wiser, MF, Lanners, HN and Bafford, RA (1999). "Export of proteins via a novel secretory pathway." Parasitol Today 15(5): 194-198.

Wyne, KL, Pathak, K, Seabra, MC and Hobbs, HH (1996). "Expression of the VLDL receptor in endothelial cells." Arterioscler Thromb Vasc Biol 16(3): 407-415.